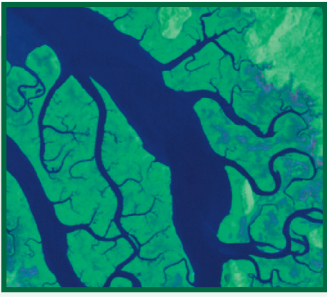
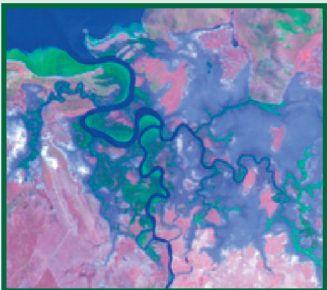


RESEARCH REPORT



Pre-processing Methodology for Application to Landsat TM/ETM+ Imagery of the Wet Tropics

Caroline M. Bruce and
David W. Hilbert



Rainforest CRC

Cooperative Research Centre for Tropical Rainforest Ecology and Management

PRE-PROCESSING METHODOLOGY FOR APPLICATION TO LANDSAT TM/ETM+ IMAGERY OF THE WET TROPICS

Caroline M. Bruce
and David W. Hilbert

CSIRO Tropical Forest Research Centre
and Rainforest CRC



Rainforest CRC



CSIRO



Established and supported under the
Australian Cooperative Research Centres Program

© Cooperative Research Centre for
Tropical Rainforest Ecology and
Management.

ISBN 0 86443 760 9

This work is copyright. The Copyright Act 1968 permits fair dealing for study, research, news reporting, criticism or review. Selected passages, tables or diagrams may be reproduced for such purposes provided acknowledgment of the source is included. Major extracts of the entire document may not be reproduced by any process without written permission of the Chief Executive Officer, CRC for Tropical Rainforest Ecology and Management.

Published by the Cooperative Research Centre for Tropical Rainforest Ecology and Management. Further copies may be requested from the Cooperative Research Centre for Tropical Rainforest Ecology and Management, James Cook University, PO Box 6811 Cairns, QLD, Australia 4870.

This publication should be cited as:
Bruce, C. M. and Hilbert, D. W. (2004)
*Pre-processing Methodology for
Application to Landsat TM/ETM+
Imagery of the Wet Tropics.*
Cooperative Research Centre for
Tropical Rainforest Ecology and
Management. Rainforest CRC,
Cairns. (44 pp.)

Compiled in July 2004.

Published by the Rainforest CRC in
March 2006.

For copies of this document please
visit www.rainforest-crc.jcu.edu.au

CONTENTS

Tables.....	ii
Figures	ii
Abstract	iii
Acknowledgements	iii
Acronyms	iv
1. Introduction	1
1.1 Background	1
1.2 Initial Image Selection	2
2. Pre-processing Methods	7
2.1 Geometric Correction and Orthorectification	7
2.2 Correction for Noise	10
2.3 Conversion to Top of Atmosphere Reflectance Units	11
2.4 Absolute Atmosphere Correction	12
2.5 Topographic Normalisation	14
2.6 Relative Radiometric Correction	17
3. References.....	19
4. Appendix: Accuracy Assessment for Landsat TM/ETM+ Imagery Used in Project 2.3	23
4.1 Geometric Correction/Orthorectification	23
4.2 Conversion of Top of Atmosphere Reflectance Units	23
4.3 Topographic Normalisation	24
4.4 Relative Radiometric Correction	38

TABLES

Table 1:	Characteristics of Landsat TM and Landsat ETM+ sensors	2
Table 2:	Characteristics of imagery available for Rainforest CRC Project 2.3	4
Table 3:	Spatial accuracy for each scene of each era expressed as Root Mean Squared (RMS) in metres, as derived from the average of a spread of Ground Control Points (GCPs)	23
Table 4:	Radiometric accuracy of each band for scenes of each era expressed as the average difference in Digital Numbers (DN) for a collection of Areas of Interest (AOI) within areas of overlap for scenes of the same date	23

FIGURES

Figure 1:	Processing procedures applied to imagery	3
Figure 2:	Ground Point Controls (GCPs) and Digital Elevation Model (DEM) used in further geometric correction of initial imagery	9
Figure 3:	Radiometric accuracy for each band for scene 9572, era 1988, expressed as the average brightness difference between spectral signatures of AOIs from both shaded and sunlit areas prior to and post topographic normalisation for representative Tracey and Webb vegetation communities as determined from Stanton and Stanton (2005)	24
Figure 4:	Radiometric accuracy for each band for scene 9573, era 1988	25
Figure 5:	Radiometric accuracy for each band for scene 9671, era 1988	26
Figure 6:	Radiometric accuracy for each band for scene 9672, era 1988	27
Figure 7:	Radiometric accuracy for each band for scene 9572, era 1994	28
Figure 8:	Radiometric accuracy for each band for scene 9573, era 1994	29
Figure 9:	Radiometric accuracy for each band for scene 9671, era 1994	30
Figure 10:	Radiometric accuracy for each band for scene 9672, era 1994	31
Figure 11:	Radiometric accuracy for each band for scene 9572, era 1999	32
Figure 12:	Radiometric accuracy for each band for scene 9573, era 1999	33
Figure 13:	Radiometric accuracy for each band for scene 9574, era 1999	34
Figure 14:	Radiometric accuracy for each band for scene 9671, era 1999	35
Figure 15:	Radiometric accuracy for each band for scene 9672, era 1999	36
Figure 16:	Radiometric accuracy for each band for scene 9673, era 1999	37
Figure 17:	Relative radiometric accuracy for each band for each mosaic, expressed as the average brightness of spectral signatures of Pseudo-Invariant Features (PIFs) spread across the 1988 and 1994 image mosaics, prior to and post radiometric correction to the 1999 image mosaic standard	38

ABSTRACT

This report details the various pre-processing techniques that are recommended for application to multispectral Landsat satellite imagery of the Queensland Wet Tropics region prior to further processing, either to derive multitemporal and multispatial image classifications or to use in biophysical/geochemical modeling. These techniques are discussed specifically as they apply to the two most recent generations of Landsat scanning sensors, Landsat Thematic Mapper (TM) and Landsat Enhanced Thematic Mapper Plus (ETM+). The techniques presented in this paper were applied to the Landsat imagery acquired by Project 2.3 of the Rainforest CRC, the outputs of which include information on landcover and its change within the Wet Tropics region. Measured biophysical properties (basal area and biomass) will also be related to the image data. The recommendations contained in this report are not specific to this project; instead, they are generally applicable to any future uses where similar outputs, in similar environments, using Landsat TM/ETM+ data are required.

Key words: remote sensing, Landsat TM, Landsat ETM+, monitoring, Queensland

ACKNOWLEDGEMENTS

Mike Peters (Geoimage, Brisbane) provided useful comments on initial pre-processing application and both Mike Linney and Ian Virtue (ACRES, Canberra) provided further information on cartographic and processing issues. Stuart Phinn (The University of Queensland, Brisbane) and Catherine Ticehurst (CSIRO Land and Water, Canberra) are particularly appreciated for their comments and critical review of this report.

ACRONYMS

ACRES	Australian Centre for Remote Sensing
AOI	Areas of Interest
CC	Cubic Convolution
CRC	Cooperative Research Centre
CSIRO	Commonwealth Scientific and Industrial Research Organisation
DEM	Digital Elevation Model
DN	Digital Number
DOS	Dark Object Subtraction
ETM+	Enhanced Thematic Mapper Plus
GCP	Ground Control Points
GPS	Global Positioning System
JCU	James Cook University
KD16	Kaiser Damped Sinc 16
MSS	Multispectral Scanner
NASA	National Aeronautics and Space Administration
NDVI	Normalised Difference Vegetation Index
NN	Nearest Neighbour
PIF	Pseudo-invariant Feature
RMS	Root Mean Squared
SLATS	Statewide Landcover and Trees Study
TFRC	Tropical Forest Research Centre
TM	Thematic Mapper
TOA	Top of Atmosphere
WTMA	Wet Tropics Management Authority

1. INTRODUCTION

The recommended pre-processing methodology for application to multispectral Landsat TM and Landsat ETM+ imagery in the Wet Tropics of Queensland or similar environments is presented within this report. These techniques are relevant to future projects where multitemporal and multispatial image classifications, or the relating of image data to measured ground attributes such as biophysical or geochemical properties, are desired. The main objectives of the report are to:

1. Evaluate the Landsat image dataset as it relates to the desired outputs of the Rainforest CRC Project 2.3;
2. Present the various pre-processing methods, considered optimal to the project's aims, that were applied to the dataset to reduce or eliminate the errors/distortions inherent in the imagery;
3. Make recommendations for the Rainforest CRC to consider in future when purchasing and pre-processing Landsat TM/ETM+ imagery for multitemporal, multispatial landcover/landuse change detection and/or biophysical/geochemical monitoring. Specific remote sensing or statistical programs that can be used in the application of procedures are also recommended. Those relating to remote sensing are restricted to the options within ERDAS Imagine, because this is a very comprehensive and powerful remote sensing software package suited to all of the pre-processing procedures defined in this report and also because ERDAS Imagine software was used to pre-process imagery for the current project.

1.1 BACKGROUND

Remotely sensed data have been widely used as a cost effective tool in the mapping and monitoring of large areas (e.g. Danaher *et al.* 1998; Gould 2000; Mayaux *et al.* 2000; Freeman *et al.* 2002). Of the many satellites that provide information useful for terrain analysis, the Landsat series has provided the longest period of coverage, spanning from the present time back to 1972 when Landsat-1 (originally known as ERTS-1) was launched. Four different types of sensors have been included in various combinations on the Landsat missions, including the Thematic Mapper (TM) present on Landsats 4 and 5, and Enhanced Thematic Mapper Plus (ETM+) present on Landsats 6 and 7. Some of the characteristics of these two sensors are outlined in Table 1.

Due to the similarity of both orbital characteristics of Landsats 4, 5 and 7 (Landsat 6 failed upon launch) and system characteristics of the TM and ETM+ sensors, data from the two sensors are largely directly comparable in terms of similar spectral, spatial, temporal and radiometric resolution. Therefore a relatively uniform time series of data dating back from the launch of Landsat 4 (16 July 1982) to the present time exists, providing an extremely useful dataset particularly for the long-term monitoring of terrestrial characteristics. The continuing production of TM data from Landsats 5 and 7 ensures the ability to directly relate the current dataset to Landsat data at least into the foreseeable future.

Before processing and analysis of the image data can occur, various pre-processing routines, appropriate to the desired output, must be applied to the imagery. These enhance the quality of the image data by reducing or eliminating various radiometric and geometric errors caused by internal and external conditions. Geometric correction procedures address errors in the relative position of pixels due to factors such as variation in altitude, attitude and velocity of the sensor platform, Earth curvature, panoramic distortion, relief displacement and non-linearities in the sweep of a sensor (Lillesand and Kiefer 1994).

Radiometric correction procedures account for errors that affect the brightness value of pixels due to both a sensor system detector error and an environmental attenuation error (e.g. changes in scene illumination, atmospheric conditions and viewing geometry [Lillesand and Kiefer 1994]). The minimisation or elimination of these errors, both between scenes and across time, is of particular importance when multitemporal or multispatial datasets are used as this allows 'normalisation' of conditions across time and space, hence direct radiometric and geometric comparison of the different images.

Table 1: Characteristics of Landsat TM and Landsat ETM+ sensors (after Lillesand and Kiefer 1994; Barrett and Curtis 1999; ACRES).

	Thematic Mapper (TM)	Enhanced Thematic Mapper Plus (ETM+)
Platform	Landsat 4 (launched 16 July 1982) Landsat 5 (launched 1 March 1984)	Landsat 6 (failed on launch) Landsat 7 (launched 15 April 1999)
Orbit	16 day/705 km	16 day/705 km
Inclination	98.2°	98.2°
Equatorial crossing time	10:00 am	10:00 am
Swath width	185 km	185 km
Bands	1 (0.45-0.52 μ m) 2 (0.52-0.60 μ m) 3 (0.63-0.69 μ m) 4 (0.76-0.90 μ m) 5 (1.55-1.75 μ m) 6 (10.4-12.5 μ m) 7 (2.08-2.35 μ m)	1 (0.45-0.52 μ m) 2 (0.52-0.60 μ m) 3 (0.63-0.69 μ m) 4 (0.76-0.90 μ m) 5 (1.55-1.75 μ m) 6 (10.4-12.5 μ m) 7 (2.08-2.35 μ m) panchromatic band 8 (0.50-0.90 μ m)
Ground pixel size	30 m (bands 1-5,7) 120 m (band 6)	30 m (bands 1-5,7) 60 m (band 6) 15 m/18 m (band 8)
Quantisation levels	8 bits	best 8 of 9 bits

After an initial assessment of the imagery obtained for use in this project, the geometric and radiometric pre-processing techniques are discussed. The procedures considered optimal to the humid tropics, the aims of Rainforest CRC Project 2.3 and to similar future monitoring projects are presented. The flowchart outlining these procedures is presented in Figure 1. For the purpose of simplicity of explanation, the pre-processing procedures have been grouped within broad categories, though it must be realised that various procedures are often applicable to several of these arbitrarily defined categories.

1.2. INITIAL IMAGE SELECTION

The initial Landsat imagery available for use within Rainforest CRC Project 2.3 was provided by different sources and had been pre-processed as outlined in Table 2. Note that although characteristics of the available Landsat MSS (Multispectral Sensor) imagery are also provided within Table 2, this imagery was not further utilised due to its incomplete coverage of the study area and the high incidence of cloud cover.

Images from all three eras had basic geometric and radiometric corrections applied initially by the Australian Centre for Remote Sensing (ACRES), then further correction for relief displacement (orthorectification) was applied by Geoimage. The processes that were applied to each dataset were therefore similar in most regards.

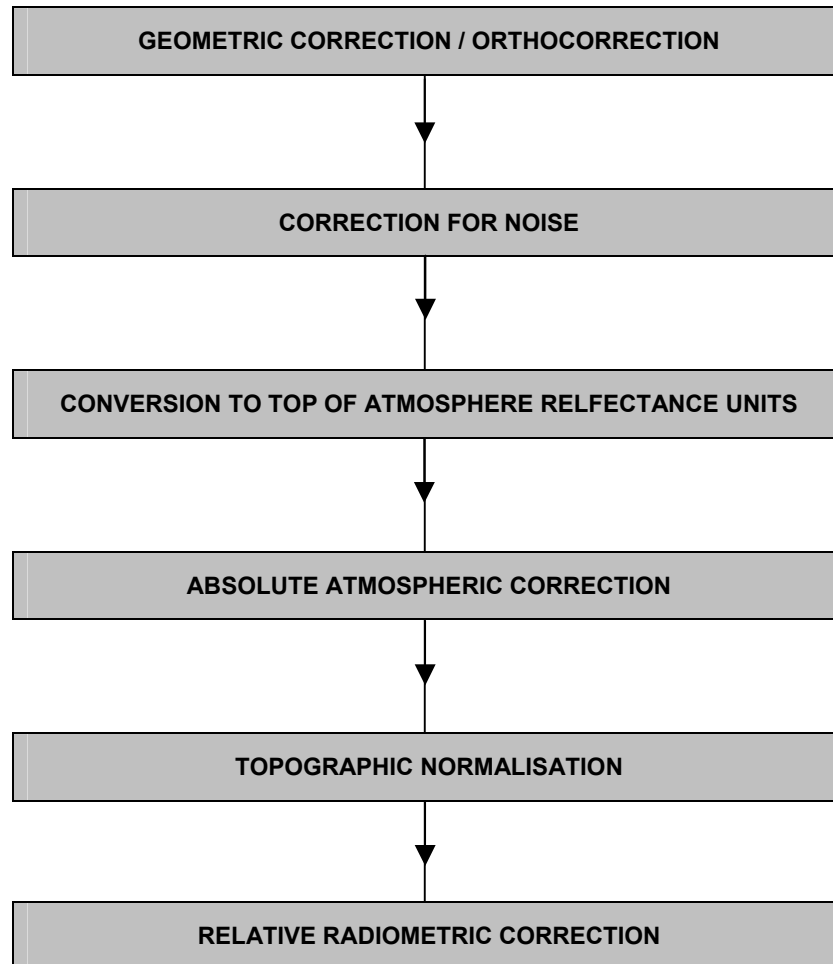


Figure 1: Processing procedures applied to imagery.

When purchasing imagery, one should ensure its suitability for the aims of the particular project by assessing the adequacy of the pre-processing applied, the suitability of the date and time of image acquisition, and the presence of brightness-degrading features in the imagery.

Appraisal of the TM/ETM+ image dataset highlighted three undesirable pre-processing features that warranted further examination. Firstly, a discrepancy existed between the nature of the resampling algorithms applied in the geometric pre-processing of the datasets by ACRES, i.e. Kaiser Damped Sinc 16 (KD16) was used to resample the 1988 and 1994 image datasets, whereas Cubic Convolution (CC) was used to resample the 1999 dataset. These resampling procedures will have altered the radiometry of the datasets in different ways; therefore they are not ideal because the application of exactly the same procedures is preferred in comparative analysis. However, according to Mike Peters from Geoimage (pers. comm.) this difference is negligible with discrepancies of up to only one Digital Number (DN) variously occurring across the images due to these different resampling algorithms. Although the discrepancy was undesirable, the minor relative difference in the resampled outputs was considered acceptable.

Secondly, the application of both the CC and KD16 algorithms means that the relative radiometric integrity of the output resampled images would have been significantly degraded. This is because both these resampling methods consider the brightness values of neighbouring pixels when computing the output value for a particular pixel, essentially 'smoothing' the output. Ideally, in applications such as Rainforest CRC Project 2.3 where image reflectance data will be related to biophysical or geochemical measurements, the radiometric integrity of the initial reflectance data for each pixel should be maintained as much as possible – this is the case because even minor changes in DN values can significantly alter relationships with biophysical/geochemical properties. By contrast, the Nearest Neighbour (NN) resampling algorithm does not consider a surrounding window and hence input spectral values are retained in the output grid. Earth scientists therefore prefer the use of this algorithm, and its application in the creation of images for this project would have been preferred. Elimination of this 'smoothing' would have required either reversal of the algorithms or a complete re-purchase of the image dataset from ACRES with just a very low level of pre-processing applied. Algorithm reversal is computationally very complex and re-purchase would have cost several thousand dollars therefore it was not an economically viable option. It was decided to accept this inherent error, however, in the acquisition of future imagery for applications where radiometric fidelity is integral to the creation of the output products, it should be ensured that wherever possible, the NN resampling algorithm is used during any pre-processing procedures applied both by the user and/or by the supplier.

Table 2: Characteristics of imagery available for Rainforest CRC Project 2.3. *

	MSS	Landsat 5 TM	Landsat 7 ETM+
Number of Images	1	4 (1988), 4 (1994)	6
Dates of Image Acquisition	August 1972	November 1988 (x2) September 1988 (x2) June 1994 (x2) September 1994 (x2)	August 1999 (x3) September 1999 (x3)
Coverage Issues	Incomplete coverage of study area; thirty percent cloud cover	Complete coverage of study area, minor cloud cover	
Pre-processing History	ACRES → Geoimage → TFRC		ACRES → DNR → Geoimage → JCU → TFRC
Pre-processing applied by ACRES	L5 (Path Image) basic corrections applied for: <ul style="list-style-type: none"> • Sensor balance (gains and offsets); • Earth rotation; • Line length; • Earth model/projection; and • Relative radiometric calibration using reference detector. 		
	Resampling algorithm used: KD16		Resampling algorithm used: CC
Pre-processing applied by Geoimage	<ul style="list-style-type: none"> • Orthorectification using a polynomial /satellite model and proprietary code, reference dataset = Raster 100,000 and Geoscience Australia's 9" DEM • Resampling algorithm used: CC 		

* Grey shading denotes imagery and pre-processing applied to the image dataset ultimately used for this project.

The final pre-processing feature requiring assessment was the orthorectification procedure applied by Geoimage. This was carried out using Geoscience Australia's 1:100,000 topographic maps and 9" Digital Elevation Model (DEM); a 250 m resolution DEM which was derived largely from 1:250,000 and 1:100,000 topographic data. Part of the aim of Rainforest CRC Project 2.3 was to create an optimally corrected image dataset using a modified version of the Wet Tropics Management Authority's (WTMA) higher-resolution DEM in our own application of both the orthorectification and other pre-processing and processing routines. As such, the fact that the dataset had already undergone orthorectification with a lesser DEM was undesirable. Fortunately, we were able to re-purchase the image dataset from Geoimage without orthorectification applied for just a few hundred dollars. This was seen as a worthwhile expense.

Hence, the image dataset ultimately used by the project comprised Landsat TM imagery (1988/1994) and Landsat ETM+ imagery (1999), both of which had had only basic pre-processing applied by ACRES. The grey shading in Table 2 denotes this imagery and the pre-processing applied to this initial dataset before Rainforest CRC Project 2.3 applied any further correction.

Beyond appraising the suitability of image pre-processing already applied, the date of image acquisition is another important consideration in the selection of an appropriate dataset. Depending on what variables are of importance to the project, imagery from certain seasons or times of the year will be desired. Usually (as was the case with CRC Project 2.3), the aim is to determine annual real change in landcover/landuse or some other variable, not changes due to seasonal conditions. Therefore, in these instances, care should be taken to ensure that image data is collected at the same time of year. Use of imagery from the same time of year also means that Earth-sun distance and solar illumination angles are consistent between dates and thus radiometric differences between dates due to these variables are also minimised. In the Wet Tropics region, the selection of data sensed during winter is also beneficial, as the ephemeral greenness that occurs mainly during the wetter summer months and that can confound the interpretation of the imagery, is not so likely to occur. If sensed in the early winter months, the imagery is also likely to have less contamination from smoke due to burning off (a feature of the autumn and later winter months). As can be seen from Table 2, it was not possible to purchase suitable imagery on anniversary dates for this project, with times of acquisition ranging from June (two 1994 images) to November (two 1998 images), i.e. a range of six months. The seasonal and ephemeral differences due to these temporal differences will have to be considered in the final analyses of the datasets.

A final consideration when selecting imagery is to ensure that it is as devoid as possible of features that degrade or mask the true ground brightness value of each pixel. This requires visual and/or statistical examination of the imagery to assess contamination by in-scene components such as clouds, smoke and haze or during data collection and transmission manifesting as line dropouts, striping and banding. Although processes can be applied to variously reduce or eliminate the effects of these contaminants, the application of such processes can be costly in terms of time and therefore money and they can also result in the removal of useful image information. Thus, the preferred method is to ensure their presence is minimised in the initial purchased imagery. Although no significant contamination due to data retrieval and transmission was apparent in the project's image datasets, cloud, smoke and haze were present to varying degrees; these were accounted for by masking (cloud and smoke) and atmospheric correction methods (haze), as discussed later in this report.

In summary, the recommendations for the Rainforest CRC to consider in the purchase of future image datasets are to:

- Purchase imagery that has been pre-processed to both an appropriate level and to the same level (if multiple images are used). Also ensure that the resampling algorithms applied during pre-processing are suitable for the aims of the project;
- Determine the optimal time/s of year when imagery should be acquired to suit the outcomes of the project; and
- Thoroughly examine available imagery and select images displaying minimal degradation due to in-scene contaminants such as cloud and smoke cover, as well as errors in the data retrieval and transmission process. Initial examination prior to purchase can often be carried out using the vendor's web-based viewing software and/or image assessment reports. Further examination and rectification after purchase can be achieved using remote sensing software such as ERDAS Imagine.

2. PRE-PROCESSING METHODS

2.1. GEOMETRIC CORRECTION AND ORTHOCORRECTION

Geometric correction had already been applied to the image datasets by ACRES as outlined in Table 2. This included application of pre-defined models to reduce the effects of Earth rotation and application of a polynomial transformation function to correct further random and residual errors, resulting in a 'map-accurate' dataset. The parameters of this transformation function were derived from a spread of Ground Control Points (GCPs) located on rasterised 1:100,000 topographic maps.

In temporal change detection, the thematic accuracy of the output is directly proportional to the product of the categorical accuracies and relative spatial accuracy of the input classified images. In turn, classification often depends on absolutely accurate image datasets in, for example, the combining of the imagery with ancillary large-scale maps to refine the classifications and/or in accuracy assessment. Such absolute accuracy is also important when relating the image data to ground-collected biophysical and/or geochemical measurements. All of the intended outputs of the current project (landcover classifications and their change over time, basal area / biomass estimates as determined from ground measurements collected with a Global Positioning System [GPS]) therefore rely on images that are geometrically as accurate as possible in both a relative and absolute sense. Ideally, sub-pixel positional accuracy is desired, however, the Landsat products, geometrically corrected to Level 5 as per the ACRES method, have positional accuracy of only +/- one kilometre (ACRES). Therefore, to produce an image dataset of sub-pixel accuracy, it was recommended that a further geometric correction procedure be applied, incorporating application of both more GCPs and a modified version of WTMA's DEM in an orthorectification procedure (Figure 2).

GCPs that would provide sub-pixel positional accuracy could potentially have been collected from maps of 1:25,000 scale and larger (GCPs from the former allowing accuracy of about twenty metres [ERDAS Inc 1995]). However, because of the extremely limited number of maps at this scale for the study area (covering only the coastal regions around Cairns, Ingham and Townsville), sub-pixel accuracy across most of the study area could only be achieved with collection and application of GPS-collected GCPs. Collection of non-differential as opposed to differential GCPs was sufficient, as this allowed horizontal accuracy to generally within fifteen metres (Garmin). Almost two hundred GCPs were collected from across and beyond the whole study area, focusing on areas of changeable relief. The two hundred GCPs included both control and check points and were used to absolutely correct geometry for all images in one era (1999). Relative correction techniques were then applied so that geometry of images in the remaining eras (1988 and 1994) were normalised to that of the absolutely corrected era. The spatial accuracies derived from this process are presented in Table 3 (Appendix 4.1)

The next step involved orthorectification with a DEM to further enhance the image geometry by accounting for the significant spatial distortion caused by relief displacement. Its application in the study area was of particular importance because of the high incidence of varied topography. Both the 3" DEM (80 m) and 9" DEM (250 m) sourced by Geoscience Australia exist for the region and were applied by the Statewide Landcover and Trees Study (SLATS) during pre-processing of their Landsat imagery to derive Statewide landcover and foliage projected cover outputs.

Preference was given to the finer resolution DEM where coverage existed (including the Wet Tropics region). These DEMs were both derived mainly from Geoscience Australia's 1:250,000 and 1:100,000 topographic mapping datasets. According to Ian Virtue from

Geoscience Australia (pers. comm.), the accuracy of these two datasets is essentially comparable, with the only appreciable difference for our purposes being grid resolution. Hence, application by SLATS of the 3" DEM should not have improved the geometry of their outputs relative to application of solely the 9" DEM.

WTMA's 80 metre DEM of the region, on the other hand, is based on the Australian Army's 1:50,000 Repromaps and is therefore significantly more accurate than Geoscience Australia's eighty-metre product. Thus, both the GPS points and a modified version of WTMA's 80 m DEM (incorporating Geoscience Australia's 9" DEM in areas where WTMA's DEM did not cover the study area, and resampled to the image pixel size of thirty metres) were applied to imagery from all three eras using ERDAS Imagine's 'Orthocorrection' function. Theoretically, after this process, the output imagery would have been distinctly superior in a geometric sense to the SLATS products.

When applying the geometric correction and relief displacement correction procedures as discussed above, the Nearest Neighbour (NN) resampling algorithm was employed so as to maintain spectral integrity.

The suggested operational sequence of events for the Rainforest CRC to follow in the geometric pre-processing of their imagery is:

1. Geometrically register each image for a selected era in the dataset using ancillary spatial data that will allow an output to the desired spatial accuracy. Both this and the subsequent relative geometric correction can be achieved with a program such as ERDAS Imagine's 'Geometric Correction' facility. Whereas GCPs from maps can be useful in initial coarse spatial rectification of the imagery, the use of GPS-derived GCPs will further enhance the spatial accuracy of the dataset and consequently that of the output products. The GCPs already collected in the field for this project can be applied to any future image dataset, where those points are visible on the imagery.
2. After absolute geometric correction of imagery for one era, relative geometric correction techniques can be used to correct the geometry of imagery from all other eras.
3. Apply orthocorrection individually to each scene in each era using a DEM of the highest planimetric accuracy possible and resampled to the grid size of the input imagery. At present, the best such DEMs available for use in the Wet Tropics region are those based on the Australian Army's 1:50,000 Repromaps (such as that produced by WTMA). Orthocorrection of TM/ETM+ imagery can be achieved within ERDAS Imagine using the 'Landsat' model within the 'Geometric Correction' facility
4. For all resampling operations (e.g. in geometric registration and orthocorrection), use the Nearest Neighbour algorithm to maintain radiometric integrity of the image.
5. Assess relative accuracy by visually examining scene overlaps both within each era and between each era. Assess absolute accuracy by relating geometrically complete product to field-collected GCPs not used in the initial geometric rectification

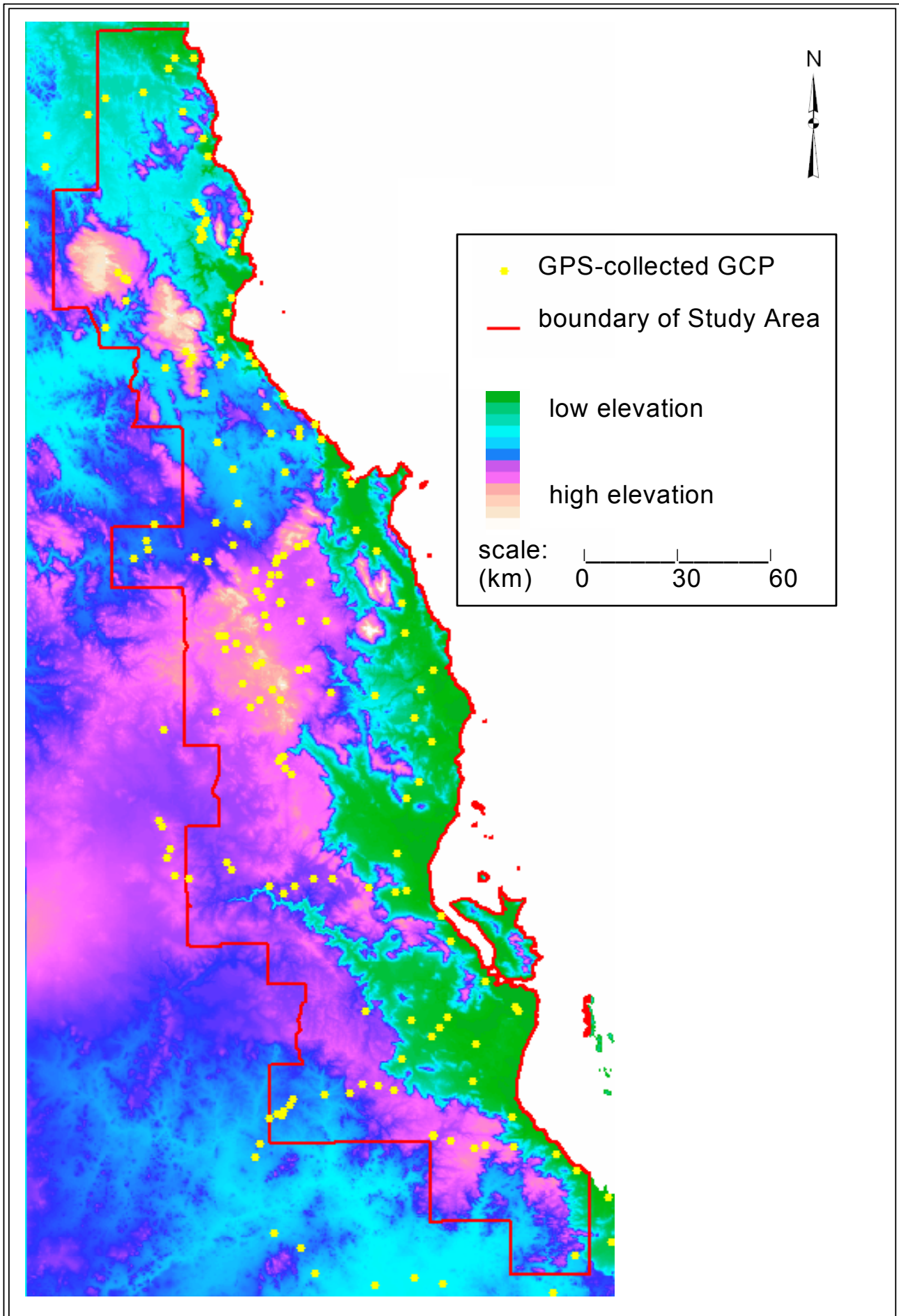


Figure 2: Ground Control Points (GCPs) and Digital Elevation Model (DEM) used in further geometric correction of initial imagery.

2.2. CORRECTION FOR NOISE

Following geometric correction of the imagery as outlined above, numerous radiometric corrections were considered for application to the imagery.

The brightness value measured for any given object is influenced by factors such as changes in scene illumination, atmospheric conditions, instrument response characteristics and viewing geometry. However the need to correct for any or all of these influences is dependent on the application at hand. In the current project, considerably more of these influences needed to be considered rather than if, for example, a single-image, broad classification was carried out. This was not just due to the outcomes of the project (classification, change detection and biophysical models), but also to the fact that a multitemporal, multispatial dataset was being used. Correcting radiometry between adjacent scenes and across time was also considered when deciding which corrections to apply.

A number of processes have been developed that attempt to account for temporal and spatial radiometric variations between scenes. They can broadly be categorised as absolute correction methods that attempt to completely remove the varying radiometric errors and produce an output absolute reflectance value for each pixel, or relative correction methods that attempt not to remove the radiometric errors, but rather to account for them by empirically correcting the radiometry of all scenes to the radiometric conditions of a reference scene. For this project, a combination of both relative and absolute methods was considered desirable to the outcomes, as discussed in the following sections.

The first radiometric error considered worthy of consideration and possible correction, was image noise produced by sensor irregularities. Noise correction partly involves calibrating the radiometry between each of the detectors, for each band, in each era. This procedure reduces much of the scan line striping inherent in imagery, produced by irregularities between the many different detectors within scanning systems. This procedure had already been applied in image pre-processing applied by ACRES and involved radiometrically matching the values from each of the detectors (generally scaled to 16 value for both Landsat 5 TM and Landsat 7 ETM+) to those of a chosen reference detector.

Examination of the imagery revealed that whereas striping due to detector differences was minor, a more obvious noise feature still present was banding, evident particularly in the 1988 and 1994 datasets. This banding is due to differences between the forward and reverse scans of the sensors, with the most obvious banding occurring in band 4 (near infrared). This difference between the forward and reverse scans was generally only 1 or 2 DN. Ideally, this differentiation should be accounted for. Helder *et al.* (1992) propose a method to reduce banding in Landsat TM by passing a one-dimensional spatial kernel over the data set. This method is applicable to radiometrically and geometrically pre-processed imagery, as is the case with the project's image dataset. However, they go on to advise that such a process can be counter-productive in terrain applications where the signal to noise ratio is high. In such applications, the noise component is negligible and its removal can involve concurrent removal of useful image detail. Crippen (1988) further cautions against the removal of scan-line noise, warning that such a process may not be suitable for data that are subsequently going to be used to extract biophysical information. The remaining scan-line noise inherent in the imagery was therefore ignored.

The imagery was examined for further systematic and random noise errors caused, for example, by detector malfunction, glitches in data transmission as well as recording and electronic interference. Such errors can manifest as line dropouts and bit errors (Lillesand and Kiefer 1994). However, visual inspection of the imagery indicated the lack of any significant degradation caused by these errors, therefore no further corrections for noise was necessary.

The suggested operational sequence of events for the Rainforest CRC to follow in the pre-processing of imagery to correct for noise is as follows:

1. Calibrate the imagery for individual detector differences if this has not already been applied. Note however that this is a standard procedure in the usual pre-processing of Landsat imagery by the image suppliers. This procedure should eliminate striping due to scan line noise. However, if striping due to detector differences or banding due to differences in the forward/reverse scans of the sensor still exist, assess their significance visually and/or statistically using software such as ERDAS Imagine and thus whether or not application of procedures for their elimination is necessary. Correct if necessary.
2. Assess the imagery for other image noise such as line dropouts and bit errors. Correct if necessary.

2.3. CONVERSION TO TOP OF ATMOSPHERE REFLECTANCE UNITS

The next process in radiometric correction involved conversion of the measured multispectral brightness values to top of atmosphere (TOA) reflectance units. This normalisation procedure is crucial when creating multitemporal and/or multispatial mosaics as it largely removes variations between these images due to sensor differences, Earth-sun distance and solar zenith angle (caused by different scene dates, overpass time and latitude differences).

The process involved two steps. The first step involved conversion of measured DN to radiance using inflight sensor calibration parameters. These parameters are supplied with the imagery and are determined from comparison of inflight calibration sources with pre-flight absolute radiance values. The exact radiometric response function for each band could therefore be determined and applied to normalise temporal radiometric differences between sensors. The equation of the response function for each band is:

Equation 1

$$L = \text{Gain} \times \text{DN} + \text{Bias}$$

where:	L	=	spectral radiance measured over spectral bandwidth of a channel
	DN	=	digital number value recorded
	Gain	=	$(L_{max} - L_{min}) / 255$ = slope of response function
	Bias	=	L_{min} = intercept of response function
	L_{max}	=	radiance measured at detector saturation in $mWcm^{-2}sr^{-1}$
	L_{min}	=	lowest radiance measured by detector in $mWcm^{-2}sr^{-1}$

The second step involved calculating top of atmosphere (TOA) reflectance for each band as per Equation 2, which corrected for illumination variations (sun angle and Earth-sun distance) within and between scenes. The correction was applied on a pixel by pixel basis for each scene in each era and the output reflectance values scaled to an 8-bit data range. Some of the parameters for the conversion are available in the image header files, while the exoatmospheric irradiance values for Landsat 5 are available from Markham and Barker (1987) and for Landsat 7 from NASA's (National Aeronautics and Space Administration) Landsat 7 Science Data Users Handbook (2003). The accuracy assessment results derived after application of the TOA equation are presented in Table 4 (Appendix 4.2).

Equation 2

$$\rho_{\lambda} = \frac{\pi d^2 L_{\lambda}}{E_{0\lambda} \cos \theta_s}$$

where:	ρ_{λ}	=	reflectance as a function of bandwidth
	d	=	Earth-sun distance correction
	L_{λ}	=	radiance as a function of bandwidth
	$E_{0\lambda}$	=	exoatmospheric irradiance
	θ_s	=	solar zenith angle

This conversion from DN to a TOA reflectance has been applied in many studies (e.g. Collet *et al.* undated; Furby undated), and according to Guyot and Gu (1994), is the most important step in the production of 'accurate' Normalised Difference Vegetation Index (NDVI) outputs, as otherwise a relatively constant error due to the sensor affects the NDVI. Other ratio indices are similarly affected. Because of its utility in estimating biomass, NDVI and other vegetation indices were to be calculated for the completed image dataset and so this conversion to TOA reflectance was necessary.

The suggested operational sequence of events for the Rainforest CRC to follow in the pre-processing of imagery to correct for sensor gains and offsets, spectral band solar irradiance and solar zenith angle is as follows:

1. Convert DN to radiance using gain and offset information for each sensor as supplied with the imagery. A modeling tool such as ERDAS Imagine's 'Spatial Modeler' can be used to define and run this and the subsequent models;
2. Convert radiance to TOA reflectance using solar zenith and Earth-sun distance values supplied with the imagery; and
3. Assess relative accuracy by comparing radiometry in pixel overlap areas for images of same date.

2.4. ABSOLUTE ATMOSPHERIC CORRECTION

Whereas the conversion from DN to TOA reflectance corrects for sensor gains and offsets spectral band solar irradiance and solar zenith angle, it makes no attempt to account for atmospheric influence. The atmosphere distorts imagery by both reducing the energy illuminating a ground object (attenuation) and by acting as a reflector itself, adding a scattered 'path radiance' component to the signal detected by a sensor (scatter). These effects are both multiplicative and additive – they differ horizontally and vertically and are also band-dependent.

The correction of these effects is not always necessary in remote sensing applications and has therefore often been ignored (Jensen 1996). However, in the current project, it was suggested that a combination of both absolute and relative correction methods be applied to account for atmospheric influence. The absolute correction was applied first, with the relative correction being applied after topographic normalisation (as described in next section).

Absolute atmospheric correction methods aim to physically account for one or more of the distorting effects of the atmosphere and thereby convert the brightness values of each pixel to actual reflectances as they would have been measured on the ground. A number of radiative transfer models such as the Tarré *et al.* (1986) 5S code, Modtran and derivatives of

these models (e.g. ACORN, FLAASH) have been developed and aim to account for these influences. These models are complex and require in-situ measurements or estimations of detailed atmospheric parameters and/or ground-based multispectral irradiance measurements to provide accurate results. No such measurements were available that related to the imagery available for the current project. However, simpler absolute correction methods derive parameters directly from the image data and some of these methods have proven to be as effective, if not more so, than the more complex radiative transfer models, in the removal of atmospheric effects (Chavez 1996; Song *et al.* 2001).

Of the image-based methods, the Dark Object Subtraction (DOS) 1% method has been successfully applied in a number of Landsat studies (Song *et al.* 2001) to remove additive path radiance, and was applied in the current project to all images in each era. This method assumes that the lowest reflectance value across a scene will be 1% for dark objects such as deep water and shadow (one or both of which occur in each image used in this project) and therefore the difference between this value and the actual DN measured for these dark objects can be attributed to the additive effects of haze. Subtraction of this value for each band will remove this error. The method is simplistic in assuming a uniform atmosphere across a scene. It accounts only for the additive effect of scattering and not the multiplicative error. However, the TM and ETM+ bands were selected to avoid measurement in the parts of the electromagnetic spectrum most prone to multiplicative scattering (Song *et al.* 2001), so this was considered not to be an issue in the current project.

Application of a method such as 'DOS 1%', which removes the additive effect of haze (rather than just normalising its influence between scenes and eras), was considered necessary for two main reasons. The first was to avoid the relatively constant error that would otherwise distort ratio indices, as mentioned in the previous section, for sensor and illumination variations. The second was to avoid the degrading or masking of the minor brightness changes between pixels due to real differences, the retention of which would be important particularly in the biophysical modeling component of the project (Jensen 1996).

After application of the 'DOS 1%' method, the output image datasets contained pixel values that approximated at-surface reflectance. A subsequent relative correction method (see Section 2.6) that normalised the reflectance of all images and hence attempted to account for any remaining atmospheric differences between images was applied after topographic normalisation (see Section 2.5). The resultant images after this relative correction were radiometrically comparable between eras and across scenes, as well as having absolute ground reflectance.

The suggested operational sequence of events for the Rainforest CRC to follow in the pre-processing of imagery to absolutely correct for atmospheric influence is as follows:

1. Remove atmospheric effect using absolute calibration method. If meteorological information exists that is relevant to the acquisition date of the image and to the area sensed, and if a working atmospheric correction model is also accessible, this should preferably be used with a suitable radiative transfer code to deduce ground reflectance. Reflectance measurements collected in-situ can also be used to derive absolute reflectance values across imagery. However, in the absence of such measurements, image-based techniques such as the 'DOS 1%' model used in the current project can be applied using a modeling tool such as ERDAS Imagine's 'Spatial Modeler'.

2.5. TOPOGRAPHIC NORMALISATION

The next correction procedure applied to the imagery attempted to account for the brightness distortion caused by differences in illumination as a result of the changing angle of the sun relative to the angle of the terrain (slope and aspect) (Smith *et al.* 1980). This correction is particularly important in the study area, as the local surface normally varies greatly due to the varied topography. The correction of these effects is termed *topographic normalisation*. According to Pons and Sole-Sugranes (1994), it is the most important of the radiometric correction procedures, as the differential effect of solar irradiance on terrain significantly varies the radiometry. Consequently, its application has been found to significantly enhance classification accuracy (Jensen 1996).

Although the study of radiometric correction of topographically induced effects is still in its relative infancy, a number of topographic normalisation correction methods exist. The simplest of these, attempts to account for radiometric differences by the use of band ratio algorithms. These have been reported to partly resolve the problem of variable illumination, provided that the atmospheric path radiance term has been eliminated (Ekstrand 1996). However, ratios have also been found to give inferior results, compared to the use of individual bands (Ekstrand 1996) and particularly to more complex procedures (Colby 1991).

These more complex procedures attempt to correct varying illumination by employing slope and aspect values and hence require a DEM of the study area. The DEM is processed so that each pixel's DN represents the amount of illumination it should receive from the sun. This information is then modeled using one of a variety of algorithms to enhance or subdue the 'original' brightness values of the image data. The DEM must be resampled to the same spatial resolution as the input imagery (Civco 1989; Furby undated; Jensen 1996). Kawata, *et al.* (1988) further state that the DEM should have the same planimetric resolution as the imagery, and according to Furby (undated), Jensen (1996) and Pons and Sole-Sugranes (1994), precise geometric correction of the DEM to the imagery is essential, otherwise misregistration can result in important over- and under-corrections on ridges and channels. These can cause severe errors in the subsequent classification stage and can also severely affect relationships derived in biophysical modeling.

The requirement for a DEM of suitable planimetric resolution has precluded the operational use of complex topographic normalisation routines in many instances, for if the slope and aspect calculated from the DEM don't match the actual terrain, the illumination corrections can cause more spectral variation than is corrected. Accordingly, Furby (undated) found that both the 9" and 3" DEMs produced by Geoscience Australia were derived from data of too small a scale to be of use in correcting nation-wide Landsat TM datasets. Naugle and Lashlee (1992) similarly showed that a DEM of ninety-five metre was insufficient for correction of Landsat TM imagery of rugged terrain.

In the current project a derivation of WTMA's DEM that was available for use, is of significantly higher topographic accuracy than Geoscience Australia's 3" DEM, being derived from 1:50,000 rather than 1:100,000 and 1:250,000 maps. Although of not the same planimetric resolution as the image data (eighty metres as opposed to thirty metres), it was hoped that the source DEM data would nonetheless be of sufficient accuracy to enhance the image radiometry to a degree, though it must be realised that a complete correction for topographic effect could not be expected.

The DEM-based topographic normalisation models presented in the literature broadly fit into two categories, depending on the assumptions about reflectance properties of the surface being sensed and therefore whether or not the surface is considered Lambertian or non-Lambertian.

The Lambertian reflectance model assumes that the surface reflects incident solar energy uniformly in all directions and that variations in reflectance are due to the amount of incident radiation (ERDAS Inc. 1995). On the other hand Non-Lambertian assumptions consider variations in the terrain and are therefore more computationally demanding than the Lambertian model and their results tend to be more accurate.

A range of studies were carried out to attempt to account for topographic effect on radiometry, most focusing on the temperate forests of the mountainous regions in the northern hemisphere. In contrast, relatively few such studies relate to mountainous tropical regions (Colby and Keating 1998). This is significant because as well as topographic attributes, the geometry of the canopy (which differs significantly between temperate and tropical forests and indeed between individual species) is thought to be a very important factor in the determination of the radiometric scattering from each pixel and hence whether or not that scattering displays Lambertian or non-Lambertian properties. As a result, findings from these temperate zone studies can not automatically be considered applicable to this study area, where rainforest and tall, wet sclerophyll vegetation types tend to dominate the areas of relief, however, no radiometric normalisation studies relating to eucalypts appear to have been published and none relate to Australia's tropical rainforests.

Many of the pioneering topographic normalisation studies focused on Lambertian models with varying results. Researchers generally found that techniques based on a Lambertian assumption were ineffective in normalising the topographic effect, except in a limited range of slope and incidence angles (Colby 1991; Colby and Keating 1998). For example Smith *et al.* (1980) found that although Lambertian models adequately accounted for radiometric variation for a limited range of incidence and exitance angles, they were generally invalid for the Ponderosa pine plantations studied. In some situations, radiometric variation actually increased. Over-correction is also noted by Jensen (1996).

However Smith *et al.* (1980) found that application of a non-Lambertian model accounted for significantly more radiometric variation across the imagery. This finding is supported by the results of a number of studies (e.g. Colby and Keating 1998) where the relative accuracy of the Minnaert constant in a non-Lambertian model has been determined. These findings are to be expected, as most objects (including forests) display non-Lambertian reflectance characteristics. For example, Meyer *et al.* (1993) determined the inaccuracy of the Lambertian model in classification of forest and reduction of visual topographic effect, relative not only to a Minnaert-based non-Lambertian algorithm, but also to statistical and C-correction approaches.

An unpublished paper by Phinn and Bailey (1998) that compared various topographic normalisation procedures, also determined better correction, based on an approach using the Minnaert constant as opposed to Lambertian models, though both approaches over-corrected shadowed areas. They further examined an approach derived by Keding (1984) and successfully applied to the correction of aerial video images by Pellikka (1996) and to the correction of Landsat TM data by Parlow (1996) and others. Phinn and Bailey (1998) applied Pellikka's (1996) adapted model to Landsat TM data covering part of the Wet Tropics region and found its performance superior to both the Lambertian and non-Lambertian models when tested visually. It was therefore decided to apply the same model in the current project.

Pellikka's (1996) model 'improves' each pixel's reflectance value based on the ratio of total irradiance (direct and diffuse) to irradiance on a horizontal surface, as per the following equation:

Equation 3

$$L_h = (E_p/E_a) \times L_t$$

where:	E_a	=	irradiance on a sloping surface
	E_p	=	irradiance on a horizontal surface
	L_h	=	slope-aspect corrected reflectance value
	L_t	=	uncorrected reflectance value

Phinn and Bailey (1998) suggest that the effectiveness of this method was due mainly to its inclusion of diffuse and direct irradiance and to the ability to control the weights applied to each spectral band in the correction model. However, they also state that its effectiveness was restricted due to the coarse size of the DEM (80 m), relative to the pixel size of the image data (25 m in this case).

Although considering both diffuse and direct irradiance, the model neglects the influence of adjacent slopes. The adjacency effect has also been ignored by other researchers who consider its effect too insignificant or complex, it was therefore ignored in the present project. Furthermore, the inability of topographic correction procedures to adequately account for shadowed areas caused by deep valleys or intervening topographic features is recognised by researchers (e.g. Meyer *et al.* 1993). It was therefore suggested that these areas be masked out using either thresholding of bands or a line-of-sight algorithm. A masking procedure was therefore applied to the project's image dataset before application of the topographic correction.

The effectiveness of the topographic correction procedure was assessed using two methods, both of which were successfully applied by Phinn and Bailey (1998) in their assessment of different normalisation routines. The first was a visual assessment of the pre- versus post-corrected images; topographic correction reduces the shadowing and brightening that characterise the appearance of variable terrain and hence their removal was expected to result in the images appearing 'flat'.

The second assessment method quantitatively assessed differences between pre- and post-corrected images by comparing signature plots of different vegetation communities, derived for both shaded and sunlit areas and as determined from Stanton and Stanton's 1:50,000 mapping (2005) of the Wet Tropics. The vegetation communities selected for this assessment were the *Closed Forest, Type 14 (Tall Open Forests and Tall Woodlands)* and *Type 16 (Medium and Low Woodlands)* classifications as defined by Tracey and Webb (1975). These spectral signatures, that for each community will exhibit lower spectral values in the shaded areas relative to the sunlit areas prior to normalisation, were expected to coincide after normalisation. The results of this assessment method are presented in Figures 3 to 16 (Appendix 4.3).

A trend towards coincidence was apparent in our project, but total coincidence did not occur for any of the vegetation communities in all bands. This suggests that the topographic normalisation had not been totally effective in removing the brightening and shading effects of topography. This result was supported by the visual analysis that showed brightening and shading still apparent in some areas, particularly where there were small-scale topographic features. This suggests that the DEM was too coarse to represent these smaller features. Another characteristic of the topographically corrected imagery, evident from visual analysis, was the occurrence of excessive over-brightening and over-shadowing on some ridges and valleys. This may also have been due to the planimetric inadequacies of the DEM, but was probably due to spatial misregistration between the imagery and DEM.

The suggested operational sequence of events for the Rainforest CRC to follow in the pre-processing of imagery to minimise topographic effects is as follows:

1. Create shadow mask using line-of-sight algorithm or thresholding. ERDAS Imagine's 'Spatial Modeler' can be used in the creation and application of both this shadow mask and of the subsequent topographic normalisation model;
2. Apply topographic normalisation using Pellikka's model and excluding shadows as defined in the shadow mask; and
3. Assess correction both by assessing removal of the visual appearance of topographic relief and by comparing the quantitative reflectance differences of similar vegetation communities in shaded and sunlit areas prior to and after normalisation.

2.6. RELATIVE RADIOMETRIC CORRECTION

Relative radiometric correction methods calibrate image reflectance to a chosen reference image and can be applied both spatially and temporally. Such relative methods are of particular importance when comparing images to detect change (Furby and Campbell 2001; Schott *et al.* 1988). In addition, the relative calibration of the images across space and time is advantageous in usually allowing direct quantitative comparison between eras and across mosaics, as long as times of year and seasonal conditions are similar (as is generally the case with the project's image dataset) (Furby undated; Schott *et al.* 1988).

Two broad strategies for relative data calibration between imagery of different dates are described in the literature, based on either data distributions or pairwise observations of pixel values. Although less sensitive to errors in geometric matching between images of different dates, the distribution-based methods such as histogram matching often rely on unreasonable data assumptions such as invariant histogram minima and maxima between image pairs (Furby and Campbell 2001). Further, the general geometric advantage was considered not to be an issue in the current project, where a spatially, highly accurate dataset had been produced. Therefore, pairwise methods were considered superior and were applied in Rainforest CRC Project 2.3.

Of the several pairwise methods, the Pseudo-invariant Feature (PIF) technique has been successfully applied in many studies (Collett *et al.* undated; Furby and Campbell 2001; Hall *et al.* 1991; Hill and Sturm 1991; Yuan and Elvidge 1996). This technique involves collection of pseudo-invariant targets (targets that exhibit minimal spectral change through time) for images in each era of interest, which are then used to derive a relationship. This relationship is subsequently used to calibrate multispatial and/or multitemporal images to a reference image, normalising for sun angle, sensor radiometry and atmospheric degradation (Furby and Campbell 2001; Schott *et al.* 1988). The pseudo-invariant targets are generally spectrally invariant man-made targets such as bitumen, concrete and other urban features, though dark vegetation and various other bright and dark features have also been used.

Schott *et al.* (1988) and Hill and Sturm (1991) warn of the limitations of the PIF technique, particularly in regard to the significant change in reflectance of assumed PIF targets that will occur due to moisture. To avoid this problem, Schott *et al.* (1988) suggests that the transformation should only be attempted when the impervious surfaces that predominate the PIF population can be assumed to be reasonably dry. In the absence of meteorological information and with the image datasets in the current project having been sensed from June to November and hence during the dry season, this will be assumed.

SLATS adopted the PIF technique in pre-processing of their statewide datasets and also found that the 'greenness' of assumed PIFs was a problem and resulted in spectral variance (Collett *et al.* undated). This problem is also recognised by Jensen (1996) and Hill and Sturm (1991). In the SLATS study, this issue arose because of the collection of non-urban, bright and dark PIFs from features such as salt pans and mine sites – areas where vegetation can grow. These sites were chosen because many of the images in their datasets did not contain urban features that are ideal sources of PIFs. The collection of such non-ideal, non-urban PIF targets was also necessary in the current project. The approach used by SLATS to minimise this problem involved collecting targets with minimum NDVI values (equating with 'greenness'). This method was adopted in the current project.

The masking out of features such as fire scars, cloud and shadow also occurred in the selection of PIFs for the current project as they can contaminate the invariant targets (Yuan and Elvidge 1996). Hill and Sturm (1991) further suggest that targets should have Lambertian reflectance characteristics and Jensen (1996) recommends the selection of targets collected at approximately the same elevation as the other land within the scene (i.e. across a range of elevations in the study area), from flat areas and also where the pattern of the target does not change in time (which suggests moisture differences).

A number of methods have been proposed for the collection of invariant PIFs, ranging from manual selection, use of iterative thresholding of bands 3 and 4 and the extraction of pixels that reside at the non-vegetated extremes of the Kauth-Thomas greenness-brightness scattergram (Hall *et al.* 1991). For the current project, it was proposed that the collection of bright and dark targets adopted by SLATS, using a combination of manual and automated thresholding methods, be extended to the collection of medium-reflectance targets as well. These were used to control the regression between the bright and dark extremes of the scattergram; an important consideration, as it avoids the assumption of a linear regression between the bright and dark PIFs that otherwise occurs (Furby and Campbell 2001).

Although the PIF technique has mostly been used for correction of time series of images, rather than spatial matching of images, by making use of the overlap region between adjoining scenes, both SLATS and CSIRO have used it to produce radiometrically matched mosaics (Collett *et al.* undated; Furby and Campbell 2001). A similar approach was adopted in the current project, thereby using the PIF techniques not only for temporal correction of scenes, but also for along-track and across-track normalisation. The resulting relative radiometric accuracy for each band for each mosaic is presented in Figure 17 (Appendix 4.4).

The suggested operational sequence of events for the Rainforest CRC to follow in the pre-processing of imagery to minimise topographic effects is as follows:

1. Mask out fire scars, clouds and smoke. ERDAS Imagine's 'Spatial Modeler' and/or 'Classifier' functions can be used to create these masks;
2. After applying the fire, cloud and smoke masks and previously created shadow mask, collect a number of PIFs in each image for each era from appropriate areas as defined above;
3. Use these PIFs to define regressions to normalise radiometry between eras as well as along and across the satellite paths. A statistical software program such as Microsoft Excel can be used to define the regressions and their parameters applied to the image data in ERDAS Imagine's 'Spatial Modeler'; and
4. Assess effectiveness of normalisation by comparing a subset of PIFs from different images and not used in the normalisation procedure. The radiometry of these PIFs should be more similar after application of the procedure. Microsoft Excel or a similar package can be used for this process also.

3. REFERENCES

ACRES Website: <http://www.auslig.gov.au/acres/>

Barrett, E. C. and Curtis, L. F. (1999). *Introduction to Environmental Remote Sensing*. 4th ed. Stanley Thornes Ltd, Glos. UK.

Chavez, P. S. Jr. (1996). Image-Based Atmospheric Corrections – Revisited and Improved. *Photogrammetric Engineering and Remote Sensing* 62(9), 1025-1036.

Civco, D. L. (1989). Topographic Normalisation of Landsat Thematic Mapper Digital Imagery. *Photogrammetric Engineering and Remote Sensing* 55(9), 1303-1309.

Colby, J. D. (1991). Topographic Normalisation in Rugged Terrain. *Photogrammetric Engineering and Remote Sensing* 57(5), 531-537.

Colby, J. D. and Keating, P. L. (1998). Land Cover Classification Using Landsat TM Imagery in the Tropical Highlands: the Influence of Anisotropic Reflectance. *International Journal of Remote Sensing* 19(8), 1479-1500.

Collett, L. J., Goulevitch, B. M. and Danaher, T. J. (undated). *SLATS Radiometric Correction: A Semi-Automated, Multi-Stage Process for the Standardisation of Temporal and Spatial Radiometric Differences*.

Crippen, R. E. (1988). The Dangers of Underestimating the Importance of Data Adjustments in Band Ratioging. *International Journal of Remote Sensing* 9(4), 767-776.

Danaher, T. J., Bisshop, G., Kastanis, L. and Carter. J. (1998). The Statewide Landcover and Trees Study (SLATS) – monitoring landcover change and greenhouse gas emissions in Queensland. *Proceedings of the 9th Australasian Remote Sensing and Photogrammetry Conference*, Sydney, Australia, July 1998.

Ekstrand, S. (1996). Landsat TM-Based Forest Damage Assessment: Correction for Topographic Effects. *Photogrammetric Engineering and Remote Sensing* 62(2), 151-161.

ERDAS Inc. (1995). *ERDAS Field Guide*, 3rd ed. ERDAS, Georgia.

Freeman, A., Chapman, B. and Siqueira, P. (2002). The JERS-1 Amazon Multi-season Mapping Study (JAMMS): Science Objectives and Implications for Future Missions. *International Journal of Remote Sensing* 23(7), 1447-1460.

Furby, S. L. and Campbell, N. A. (2001). Calibrating Images from Different Dates to 'Like-Value' Digital Counts. *Remote Sensing of Environment* 77, 186-196.

Furby, S. (undated). *Technical Report 9. Land Cover Change: Specifications for Remote Sensing Analysis*. <http://www.greenhouse.gov.au/ncas/files/pdfs/tr09appx.pdf>

Garmin. Website: <http://www.garmin.com/aboutGPS/>

Gould, W. (2000). Remote Sensing of Vegetation, Plant Species Richness and Regional Biodiversity Hotspots. *Ecological Applications* 10(6), 1861-1870.

Guyot, G. and Gu, X. (1994). Effect of Radiometric Corrections on NDVI-Determined from SPOT-HRV and Landsat-TM Data. *Remote Sensing of Environment* 49,169-180.

Hall, F. G., Strebel, D. E., Nickeson, J. E. and Goetz, S. J. (1991). Radiometric Rectification: Toward a Common Radiometric Response Among Multidate, Multisensor Images. *Remote Sensing of Environment* 35, 11-27.

Helder, D. L., Quirk, B. K. and Hood, J. J. (1992). A Technique for the Reduction of Banding in Landsat Thematic Mapper Images. *Photogrammetric Engineering and Remote Sensing* 58(10), 1425-1431

Hill, J. and Sturm, B. (1991). Radiometric Correction of Multitemporal Thematic Mapper Data for Use in Agricultural Land-cover Classification and Vegetation Monitoring. *International Journal of Remote Sensing* 12(7), 1471-1491

Jensen, J. R. (1996). *Introductory Digital Image Processing – a Remote Sensing Perspective*, Prentice Hall, Englewood Cliffs, N.J.

Kawata, Y., Ueno, S. and Kusaka, T. (1988). Radiometric Correction for Atmospheric and Topographic Effects on Landsat MSS Images. *International Journal of Remote Sensing* 9, 729-748.

Keding, I. (1984). *Die räumliche Verteilung der effektiven Sonneneinstrahlung in Gebirge*. Diploma thesis, Institute of Physical Geography, University Freiburg.

Lillesand, T. M. and Kiefer, R. W. (1994). *Remote Sensing and Image Interpretation*, 3rd ed. John Wiley and Sons, New York.

Markham, B. L. and Barker, J. L. (1987). Thematic Mapper Bandpass Solar Exoatmospheric Irradiances. *International Journal of Remote Sensing* 8(3), 517-523.

Mayaux, P., De Grandi, G. and Malingreau, J. P. (2000). Central African Forest Cover Revisited: A Multisatellite Analysis. *Remote Sensing of Environment* 71(2), 183-196.

Meyer, P., Itten, K. I., Kellenberger, T., Sandmeier, S. and Sandmeier, R. (1993). Radiometric Corrections of Topographically Induced Effects on Landsat TM Data in an Alpine Environment. *ISPRS Journal of Photogrammetry and Remote Sensing* 48(4), 17-28.

NASA. (2003). *Landsat 7 Science Data Users Handbook*. Website: http://ltpwww.gsfc.nasa.gov/IAS/handbook/handbook_toc.html

Naugle, B. I. and Lashlee, J. D. (1992). Alleviating Topographic Influences on Land-cover Classifications for Mobility and Combat Modeling. *Photogrammetric Engineering and Remote Sensing* 58(8), 1217-1221

Parlow, E. (1996). Correction of Terrain Controlled Illumination Effects in Satellite Data. *Progress in Environmental Remote Sensing Research and Applications*, Parlow (ed), Balkema, Rotterdam.

Pellikka, P. (1996). Illumination Compensation for Aerial Video Images to Increase Land Cover Classification Accuracy in Mountains. *Canadian Journal of Remote Sensing* 22(4), 368-381.

Phinn, S. and Bailey, L. (1998). *Forest Clearing and Recovery Assessment from Landsat Thematic Mapper Image Data for the Wet Tropics Management Area: A Summary Report* Prepared for: Wet Tropics Management Authority

Pons, X. and Sole-Sugranes, L. (1994). A Simple Radiometric Correction Model to Improve Automatic Mapping of Vegetation from Multispectral Satellite Data. *Remote Sensing of Environment* 48, 191-204

Schott, J. R., Salvaggio, C. and Volchok, W. J. (1988). Radiometric Scene Normalisation Using Pseudoinvariant Features. *Remote Sensing of Environment* 26, 1-16.

Smith, J. A., Tzeu L. L., and Ranson, K. J. (1980). The Lambertian Assumption and Landsat Data. *Photogrammetric Engineering and Remote Sensing* 46 (9), 1183-1189.

Song, C., Woodcock, C. E., Seto, K. C., Lenney, M. P. and Scott, A. M. (2001). Classification and Change Detection Using Landsat TM Data: When and How to Correct Atmospheric Effects? *Remote Sensing of Environment* 75, 230-244.

Stanton J. P. and Stanton D. J. (2005) *Vegetation of the Wet Tropics of Queensland bioregion*. Wet Tropics Management Authority, Cairns.

Tanré, D., Deroo, C., Duhaut, P., Herman, M., Morerette, J. J., Perbos, J. and Deschamps, P.Y. (1986). Description of a Computer Code to Simulate the Satellite Signal in the Solar Spectrum: the 5S Code. *International Journal of Remote Sensing* 11(4), 659-668.

Tracey, J. G. and Webb, L. J. (1975). *Vegetation of the Humid Tropical Region of North Queensland. (15 maps at 1:100,000 scale + key.)* CSIRO Aust. Long Pocket Labs: Indooroopilly, Qld.

Yuan, D. and Elvidge, C. D. (1996). Comparison of Relative Radiometric Normalisation Techniques. *ISPRS Journal of Photogrammetry and Remote Sensing* 51, 117-126.

4. APPENDIX – ACCURACY ASSESSMENT FOR LANDSAT TM/ETM+ IMAGERY USED IN PROJECT 2.3.

4.1. GEOMETRIC CORRECTION/ORTHOCORRECTION

Table 3: Spatial accuracy for each scene of each era expressed as a Root Mean Square (RMS) in metres, as derived from the average of a spread of check Ground Control Points (GCPs).

	9572	9573	9574	9671	9672	9673
1999 (absolute)						
X RMS (+/-)	16.9	24.9	11.5	25.8	21.1	8.9
Y RMS (+/-)	13.6	13.1	7.1	13.1	14.5	16.7
TOTAL RMS (+/-)	21.6	28.1	13.5	29.0	25.6	18.9
1994 (relative to 1999)						
X RMS (+/-)	14.9	14.5		14.3	17.4	
Y RMS (+/-)	12.8	12.9		13.3	9.8	
TOTAL RMS (+/-)	19.6	19.3		19.5	20.0	
1988 (relative to 1999)						
X RMS (+/-)	14.9	15.2		14.8	17.1	
Y RMS (+/-)	11.0	12.8		12.7	10.0	
TOTAL RMS (+/-)	18.5	19.9		19.5	19.8	
N.B. Estimated accuracy ACRES orthorectified products (L5/L7) = +/- 60m						

4.2. CONVERSION TO TOP OF ATMOSPHERE (TOA) REFLECTANCE UNITS

Table 4: Radiometric accuracy of each band for scenes of each era expressed as the average difference in Digital Numbers (DN) for a collection of Areas of Interest (AOI) within areas of overlap for scenes of the same date.

	B1	B2	B3	B4	B5	B6
1999						
9671 - 9672	-0.03	-0.09	-0.09	-0.15	-0.24	-0.15
9672 - 9673	0.12	0.19	0.21	-0.17	0.30	0.04
9572 - 9573	-0.02	0.02	-0.01	-0.04	-0.04	-0.03
9573 - 9574	0.06	-0.07	-0.11	-0.19	-0.18	-0.18
1994						
9671 - 9672	-0.17	-0.13	0.06	0.35	0.43	0.19
9572 - 9573	-0.02	0.12	0.14	0.40	0.05	0.12
1988						
9671 - 9672	0.01	0.09	0.21	0.26	0.27	0.11
9572 - 9573	0.16	0.11	0.18	0.47	0.06	0.25

4.3. TOPOGRAPHIC NORMALISATION

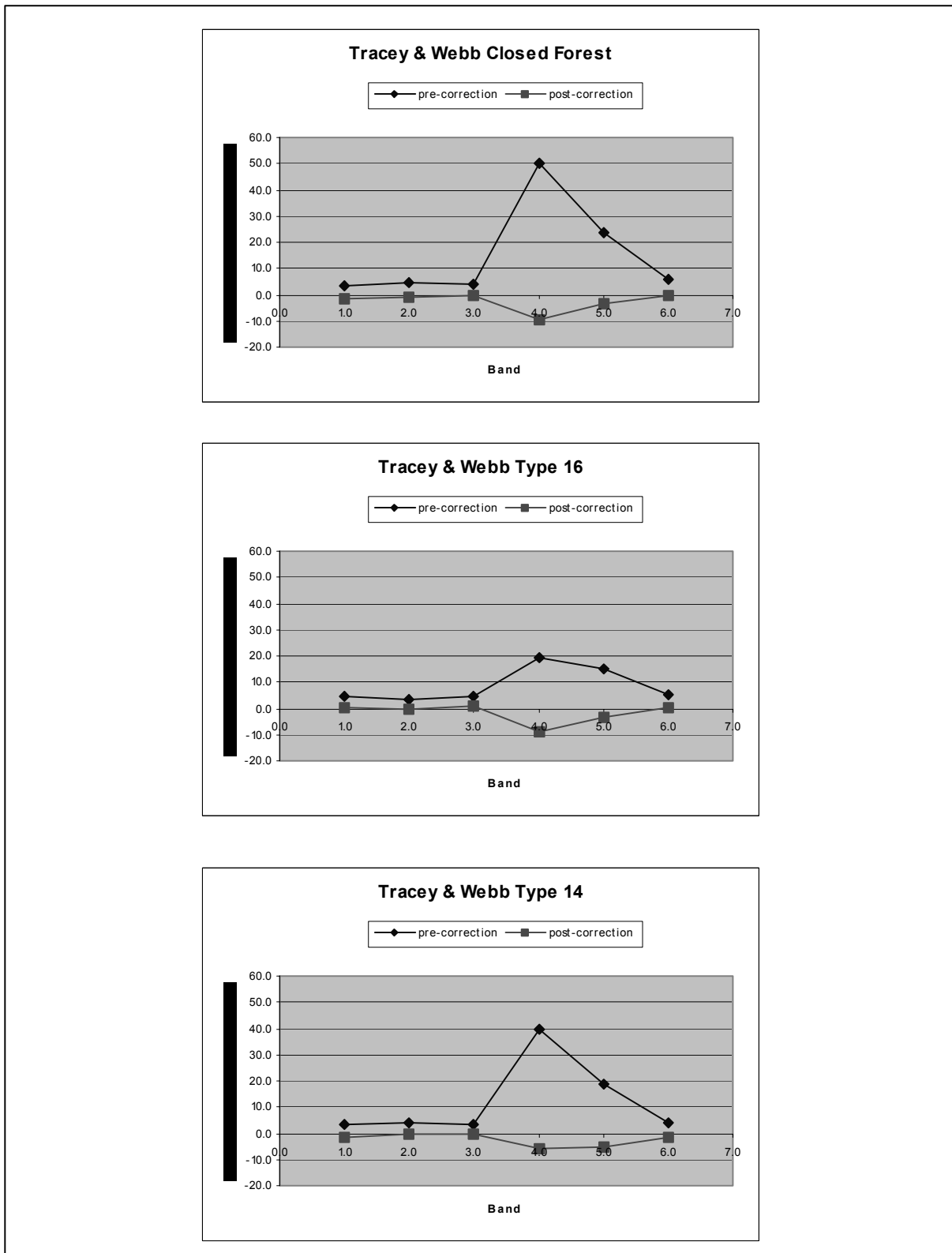


Figure 3: Radiometric accuracy for each band for scene 9572, era 1988, expressed as the average brightness difference between spectral signatures of Areas of Interest (AOIs) from both shaded and sunlit areas prior to and post topographic normalisation, for representative Tracey and Webb vegetation communities as determined from Stanton and Stanton (2005).

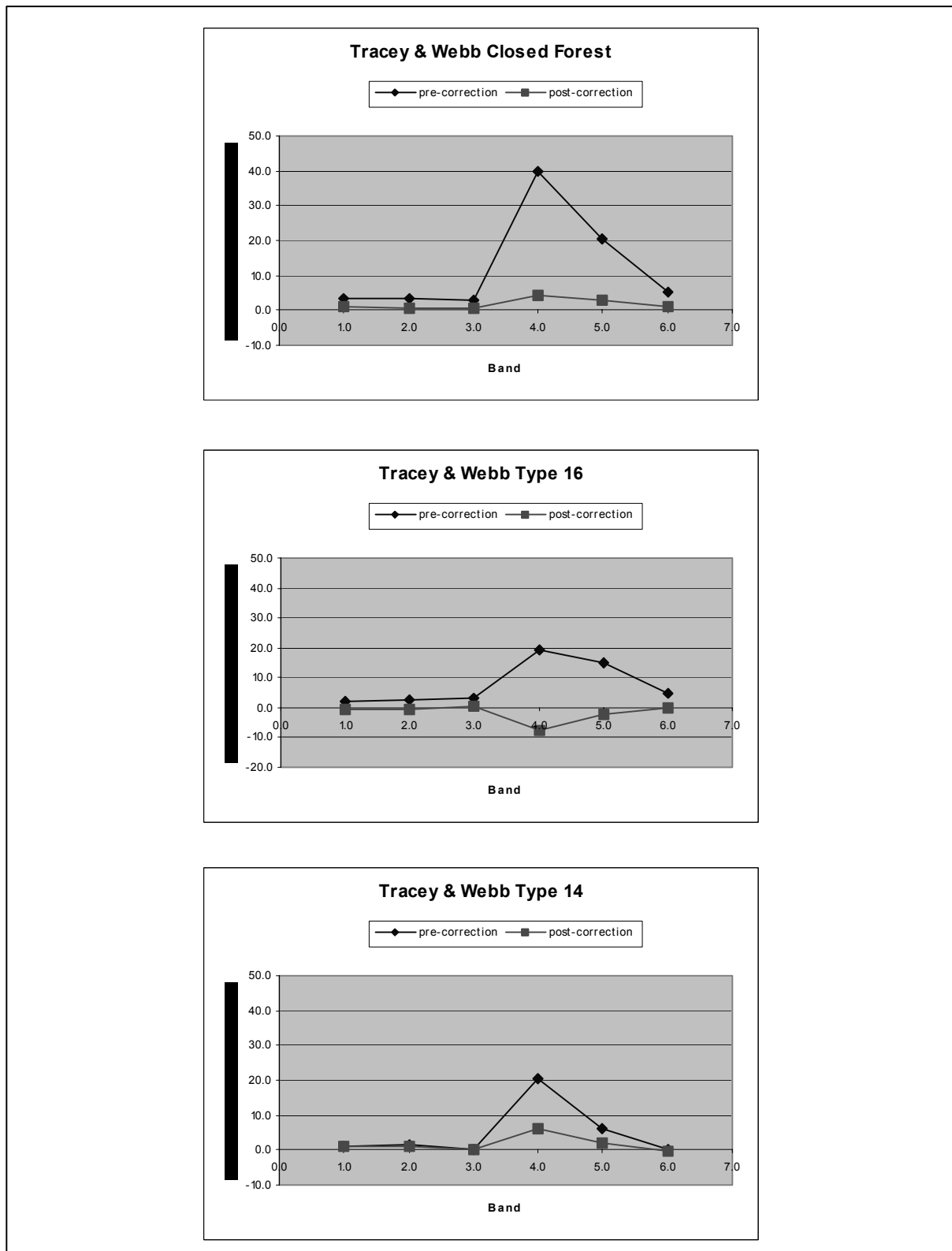


Figure 4: Radiometric accuracy for each band for scene 9573, era 1988, expressed as the average brightness difference between spectral signatures of Areas of Interest (AOIs) from both shaded and sunlit areas prior to and post topographic normalisation, for representative Tracey and Webb vegetation communities as determined from Stanton and Stanton (2005).

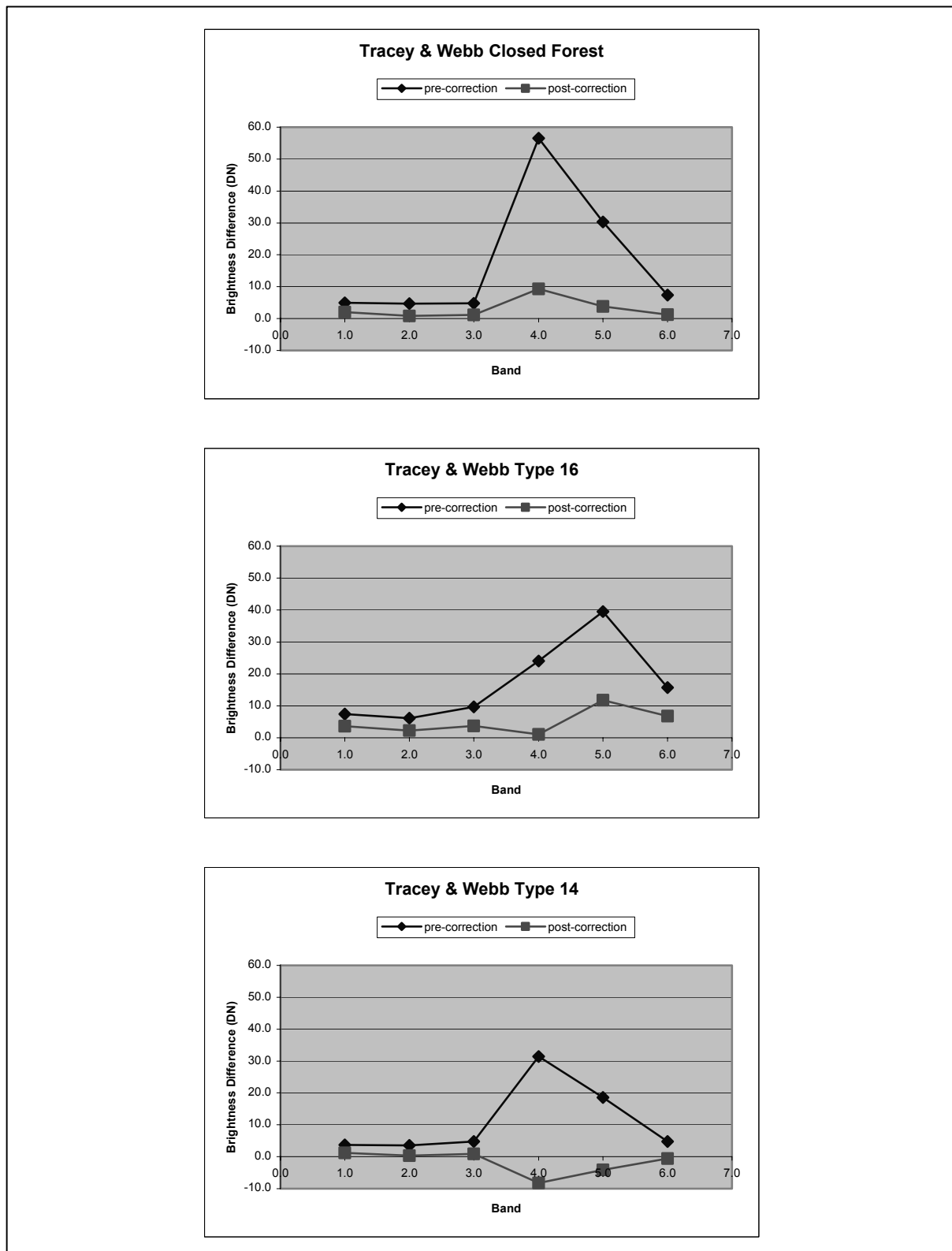


Figure 5: Radiometric accuracy for each band for scene 9671, era 1988, expressed as the average brightness difference between spectral signatures of Areas of Interest (AOIs) from both shaded and sunlit areas prior to and post topographic normalisation, for representative Tracey and Webb vegetation communities as determined from Stanton and Stanton (2005).

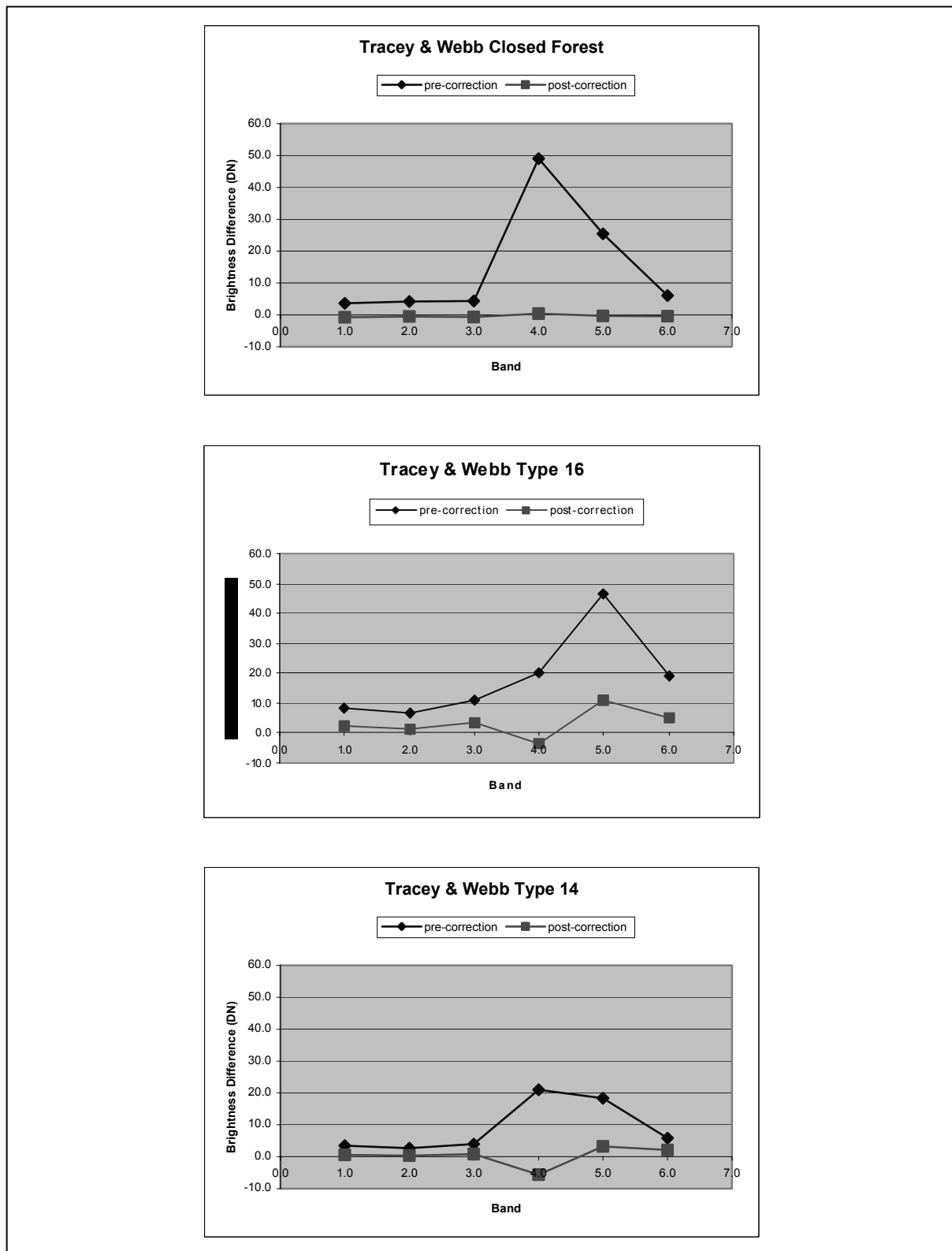


Figure 6: Radiometric accuracy for each band for scene 9672, era 1988, expressed as the average brightness difference between spectral signatures of Areas of Interest (AOIs) from both shaded and unlit areas prior to and post- topographic normalisation, for representative Tracey and Webb vegetation communities as determined from Stanton and Stanton (2005).

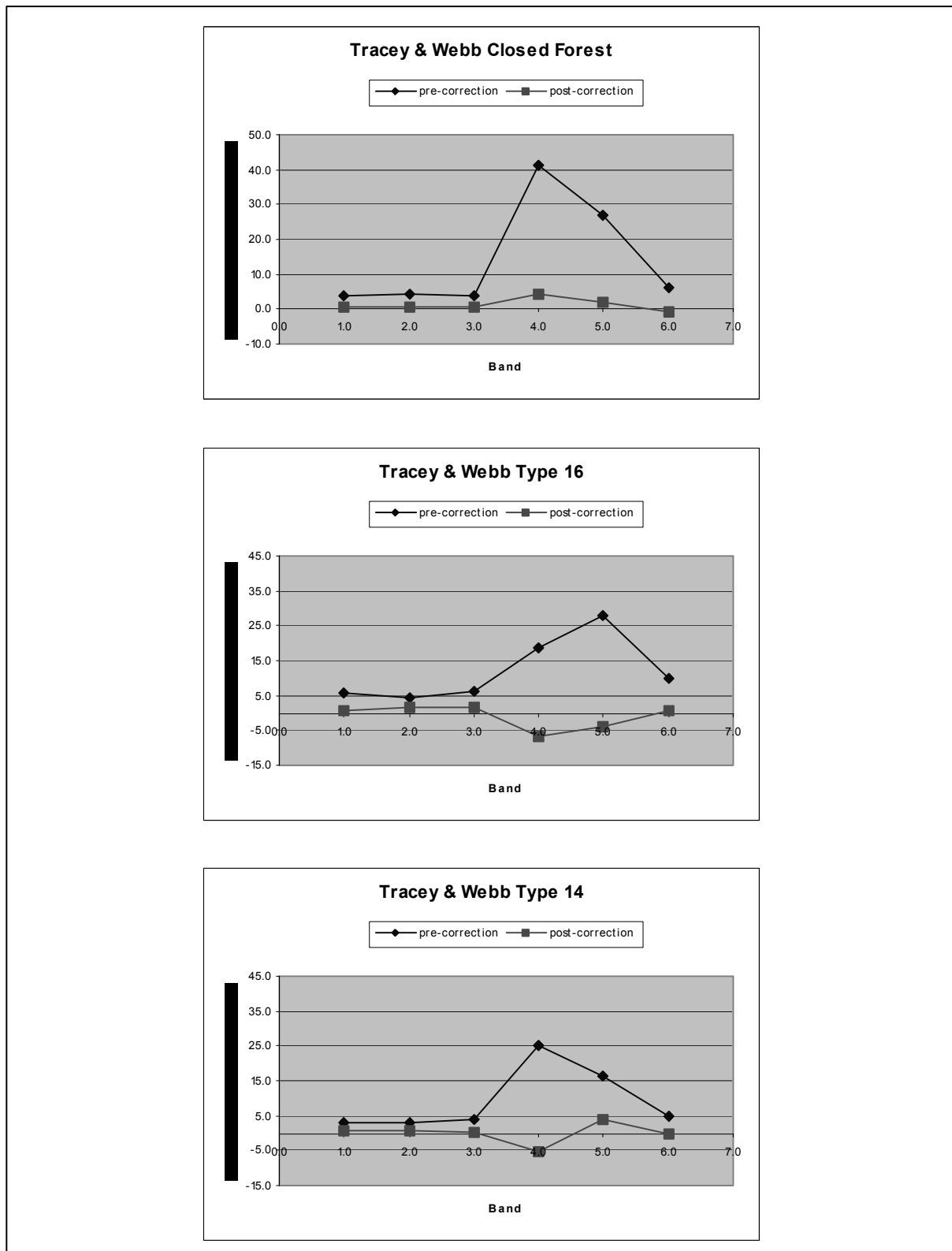


Figure 7: Radiometric accuracy for each band for scene 9572, era 1994, expressed as the average brightness difference between spectral signatures of Areas of Interest (AOIs) from both shaded and sunlit areas prior to and post topographic normalisation, for representative Tracey and Webb vegetation communities as determined from Stanton and Stanton (2005).

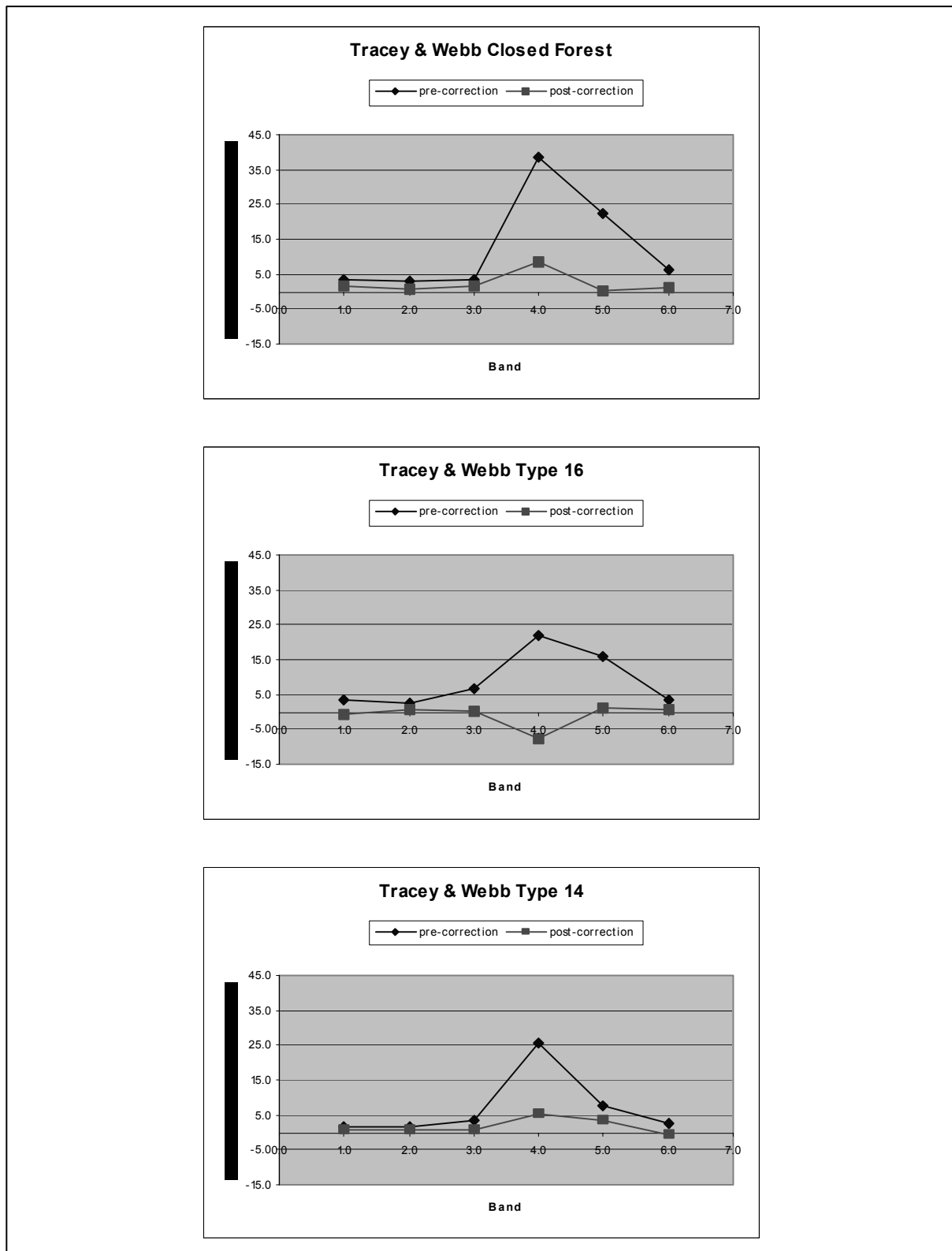


Figure 8: Radiometric accuracy for each band for scene 9573, era 1994, expressed as the average brightness difference between spectral signatures of Areas of Interest (AOIs) from both shaded and sunlit areas prior to and post topographic normalisation, for representative Tracey and Webb vegetation communities as determined from Stanton and Stanton (2005).

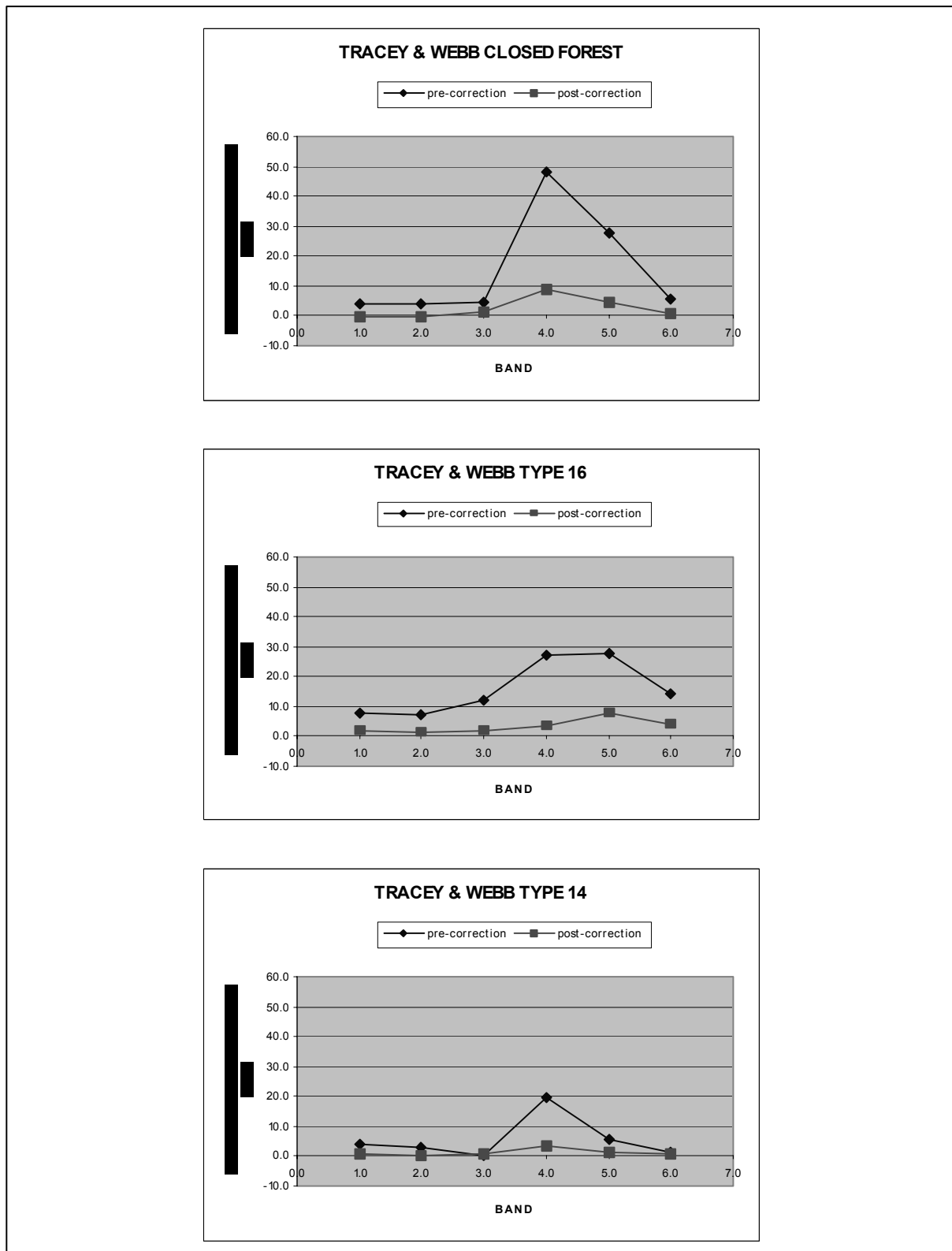


Figure 9: Radiometric accuracy for each band for scene 9671, era 1994, expressed as the average brightness difference between spectral signatures of Areas of Interest (AOIs) from both shaded and sunlit areas prior to and post topographic normalisation, for representative Tracey and Webb vegetation communities as determined from Stanton and Stanton (2005).

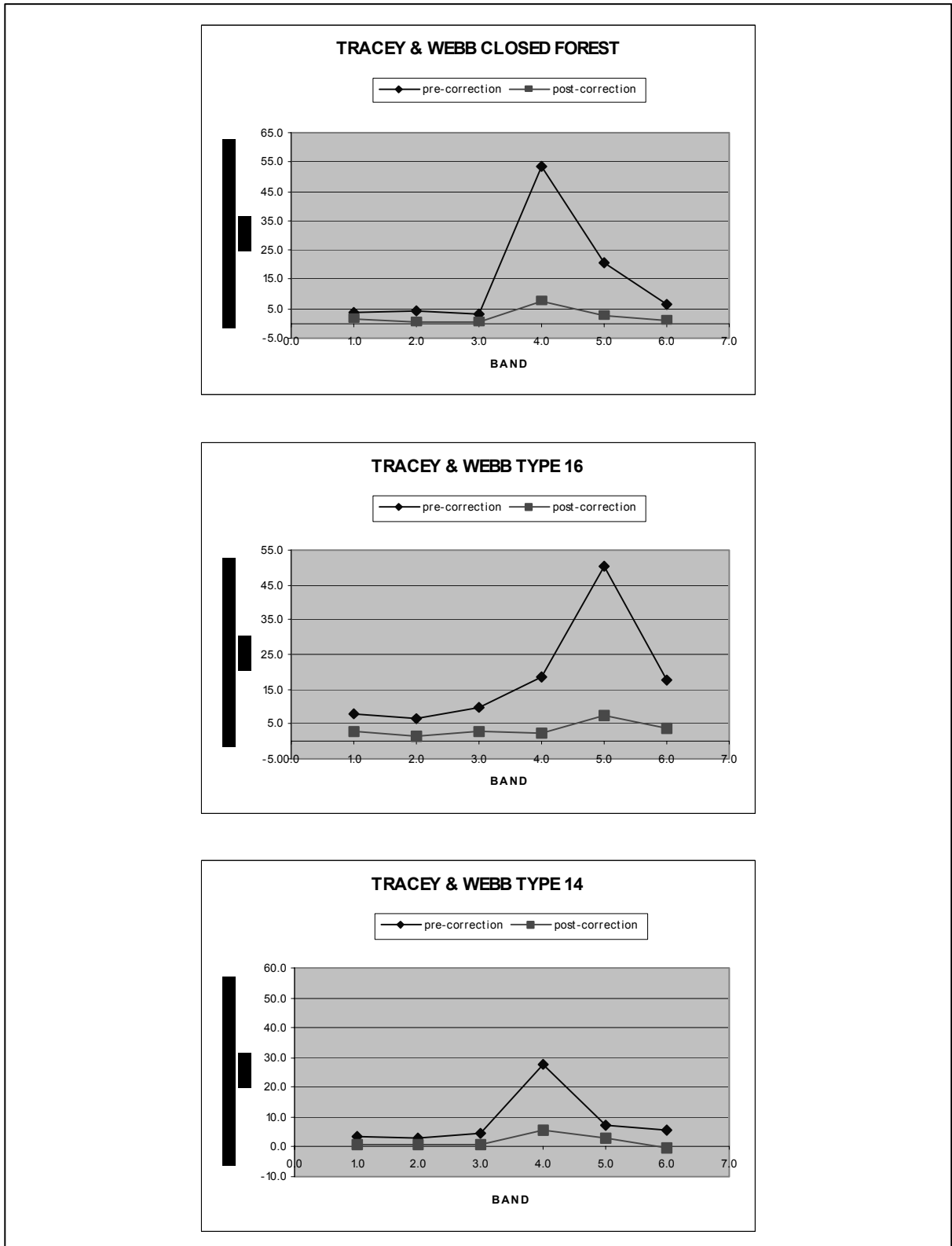


Figure 10: Radiometric accuracy for each band for scene 9672, era 1994, expressed as the average brightness difference between spectral signatures of Areas of Interest (AOIs) from both shaded and sunlit areas prior to and post topographic normalisation, for representative Tracey and Webb vegetation communities as determined from Stanton and Stanton (2005).

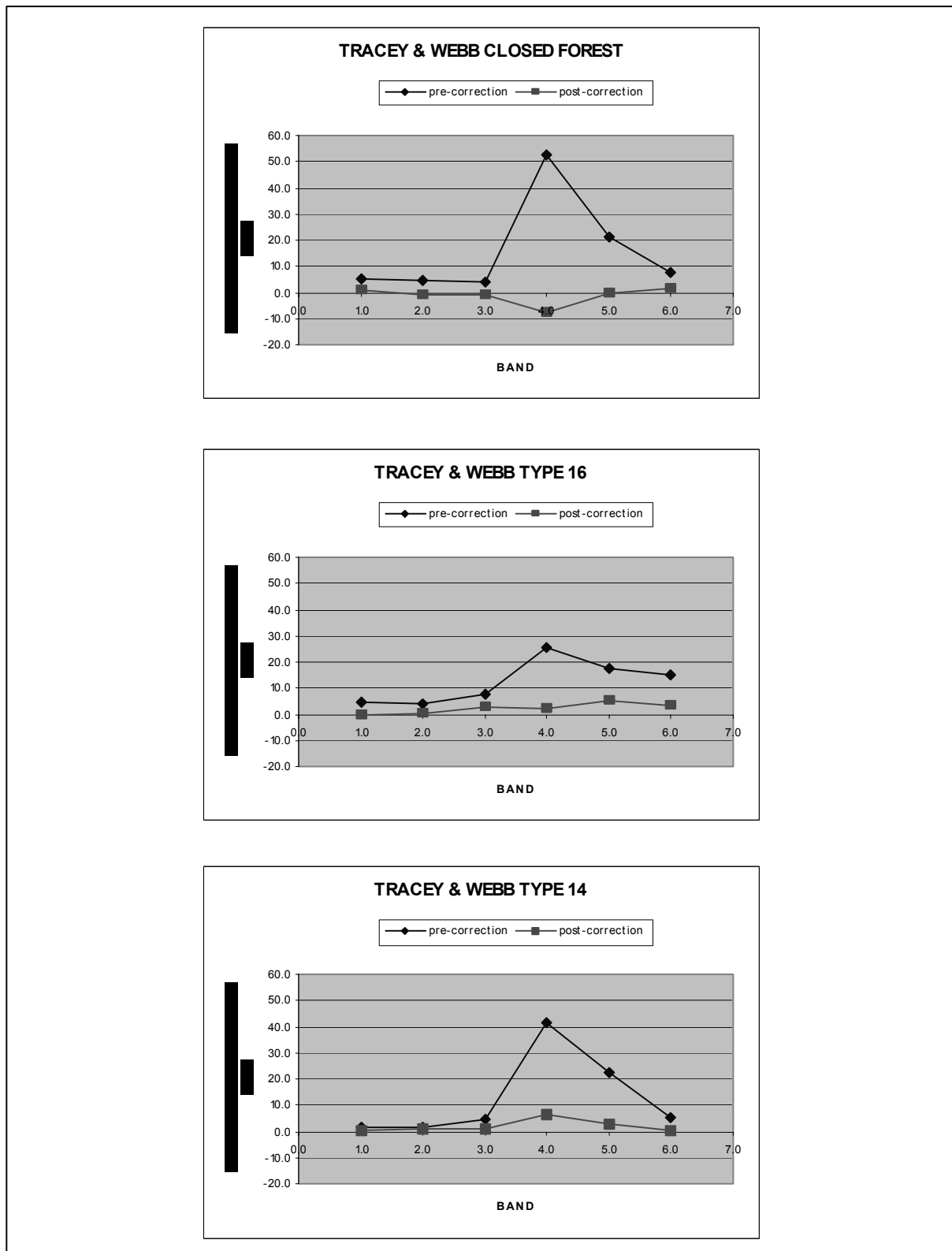


Figure 11: Radiometric accuracy for each band for scene 9572, era 1999, expressed as the average brightness difference between spectral signatures of Areas of Interest (AOIs) from both shaded and sunlit areas prior to and post topographic normalisation, for representative Tracey and Webb vegetation communities as determined from Stanton and Stanton (2005).

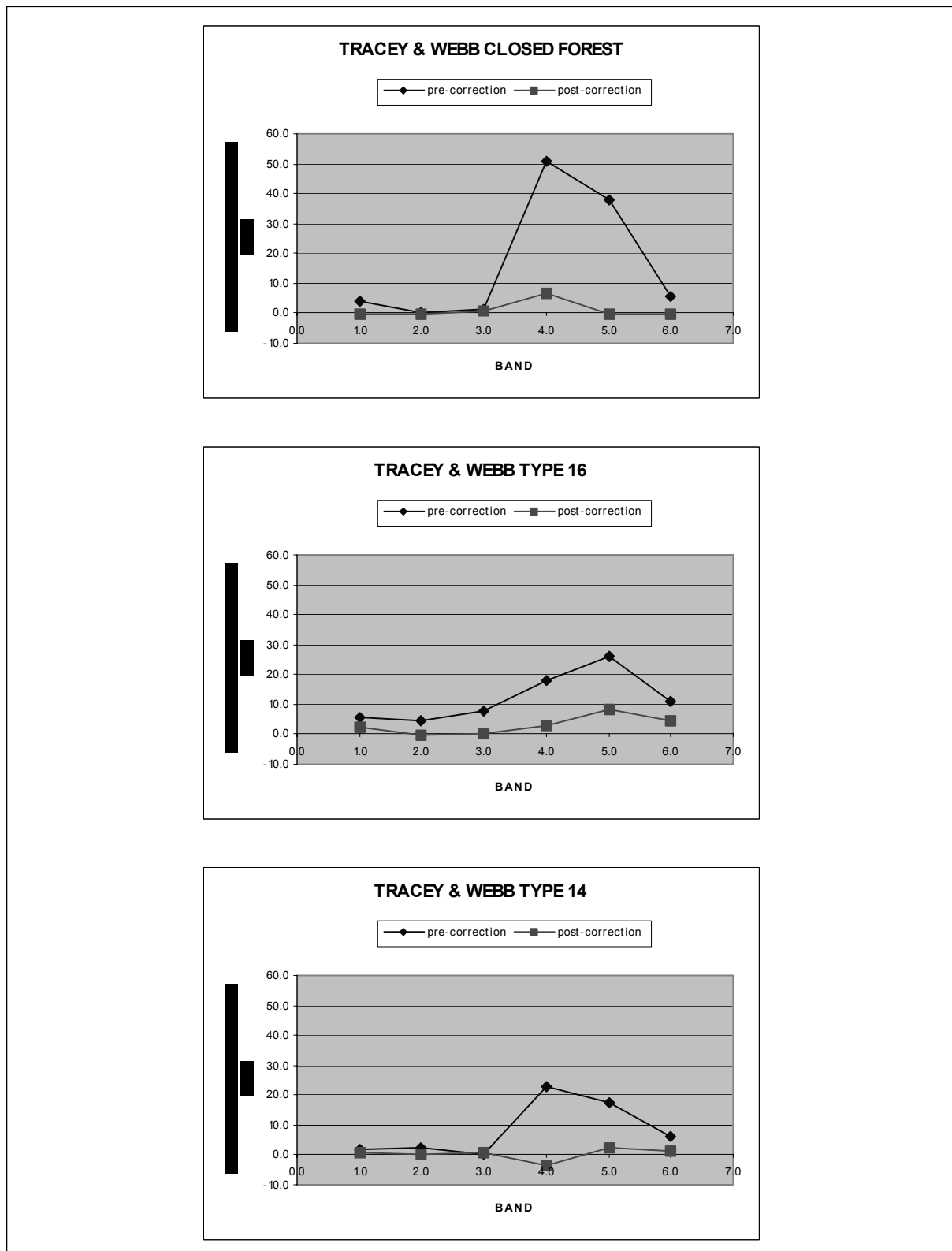


Figure 12: Radiometric accuracy for each band for scene 9573, era 1999, expressed as the average brightness difference between spectral signatures of Areas of Interest (AOIs) from both shaded and sunlit areas prior to and post topographic normalisation, for representative Tracey and Webb vegetation communities as determined from Stanton and Stanton (2005).

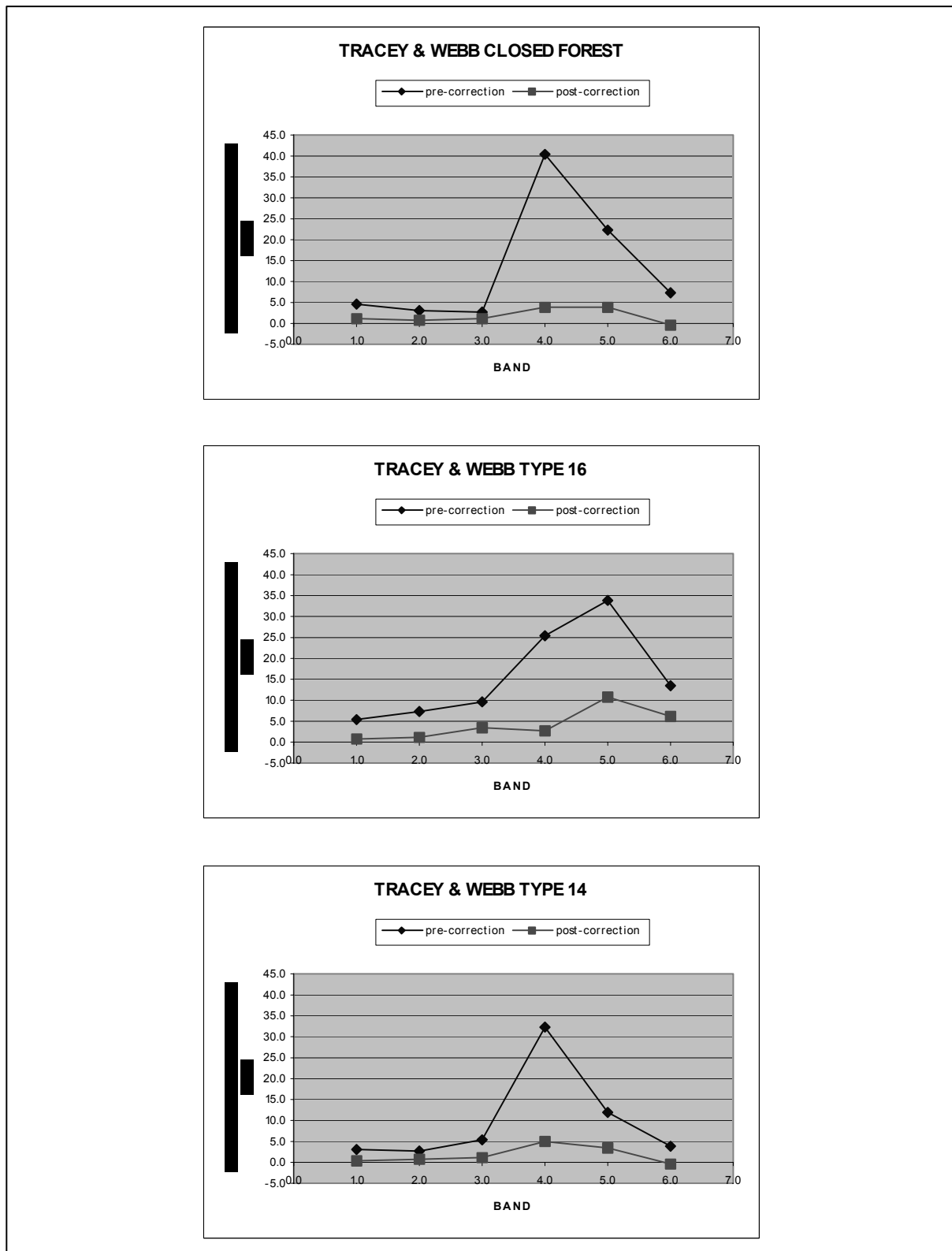


Figure 13: Radiometric accuracy for each band for scene 9574, era 1999, expressed as the average brightness difference between spectral signatures of Areas of Interest (AOIs) from both shaded and sunlit areas prior to and post topographic normalisation, for representative Tracey and Webb vegetation communities as determined from Stanton and Stanton (2005).

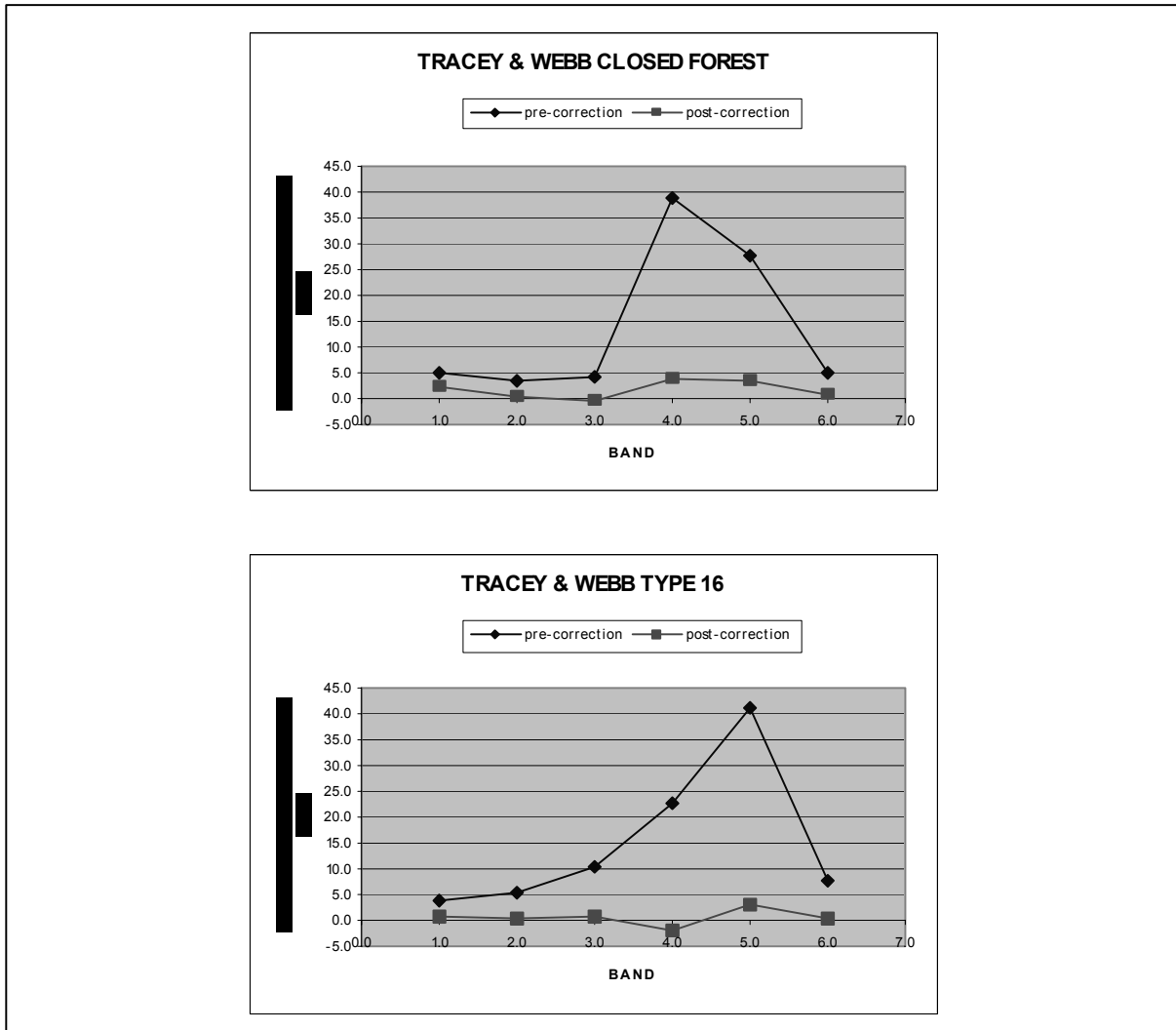


Figure 14: Radiometric accuracy for each band for scene 9671, era 1999, expressed as the average brightness difference between spectral signatures of Areas of Interest (AOIs) from both shaded and sunlit areas prior to and post topographic normalisation, for representative Tracey and Webb vegetation communities as determined from Tracey and Webb (1975). Note, the Stanton and Stanton (2005) mapping available at the time of this study did not cover this scene. Instead Tracey and Webb (1975) mapping was used for assessment. Further, Tracey and Webb Type 14 vegetation does not occur within this scene.

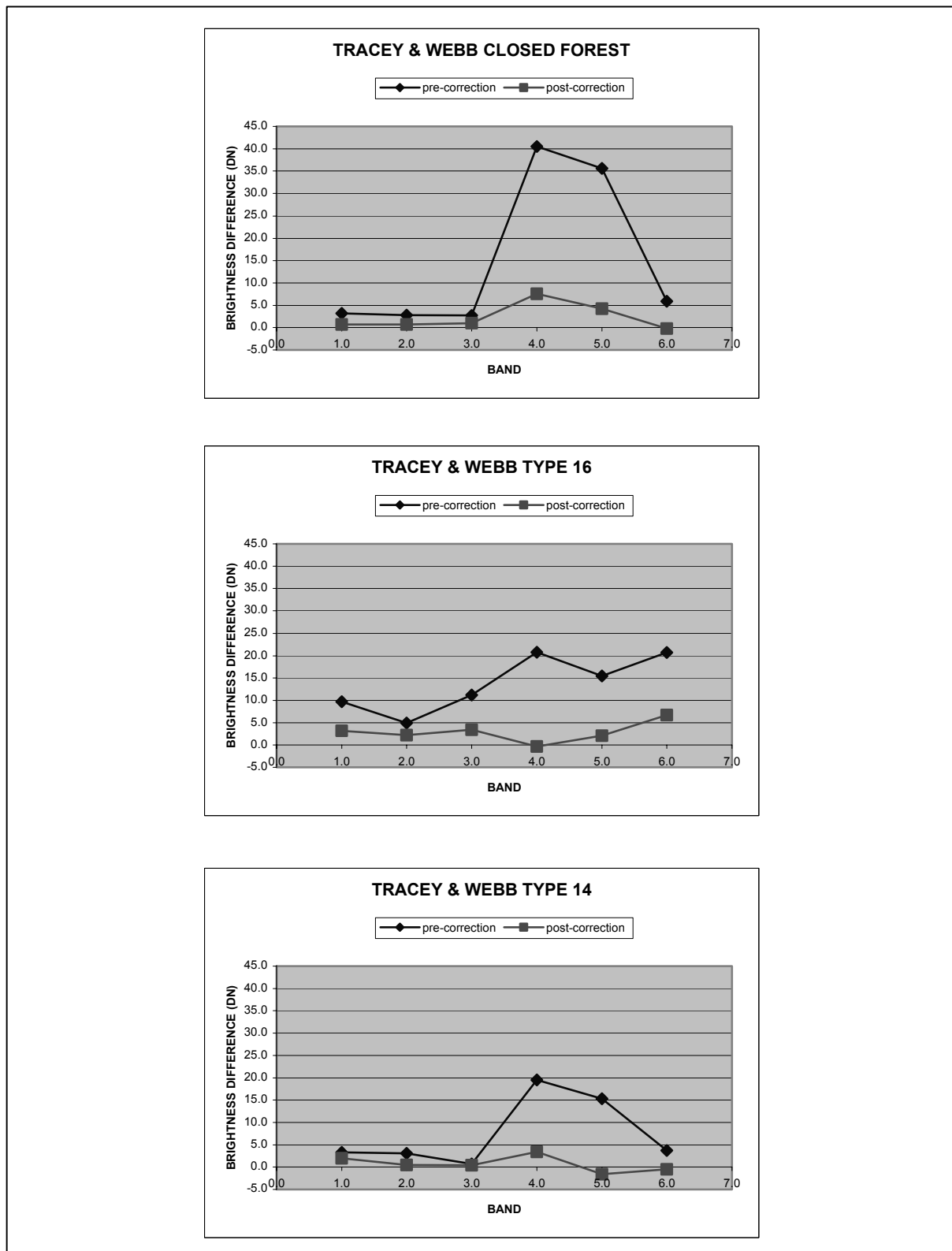


Figure 15: Radiometric accuracy for each band for scene 9672, era 1999, expressed as the average brightness difference between spectral signatures of Areas of Interest (AOIs) from both shaded and sunlit areas prior to and post topographic normalisation, for representative Tracey and Webb vegetation communities as determined from Stanton and Stanton (2005).

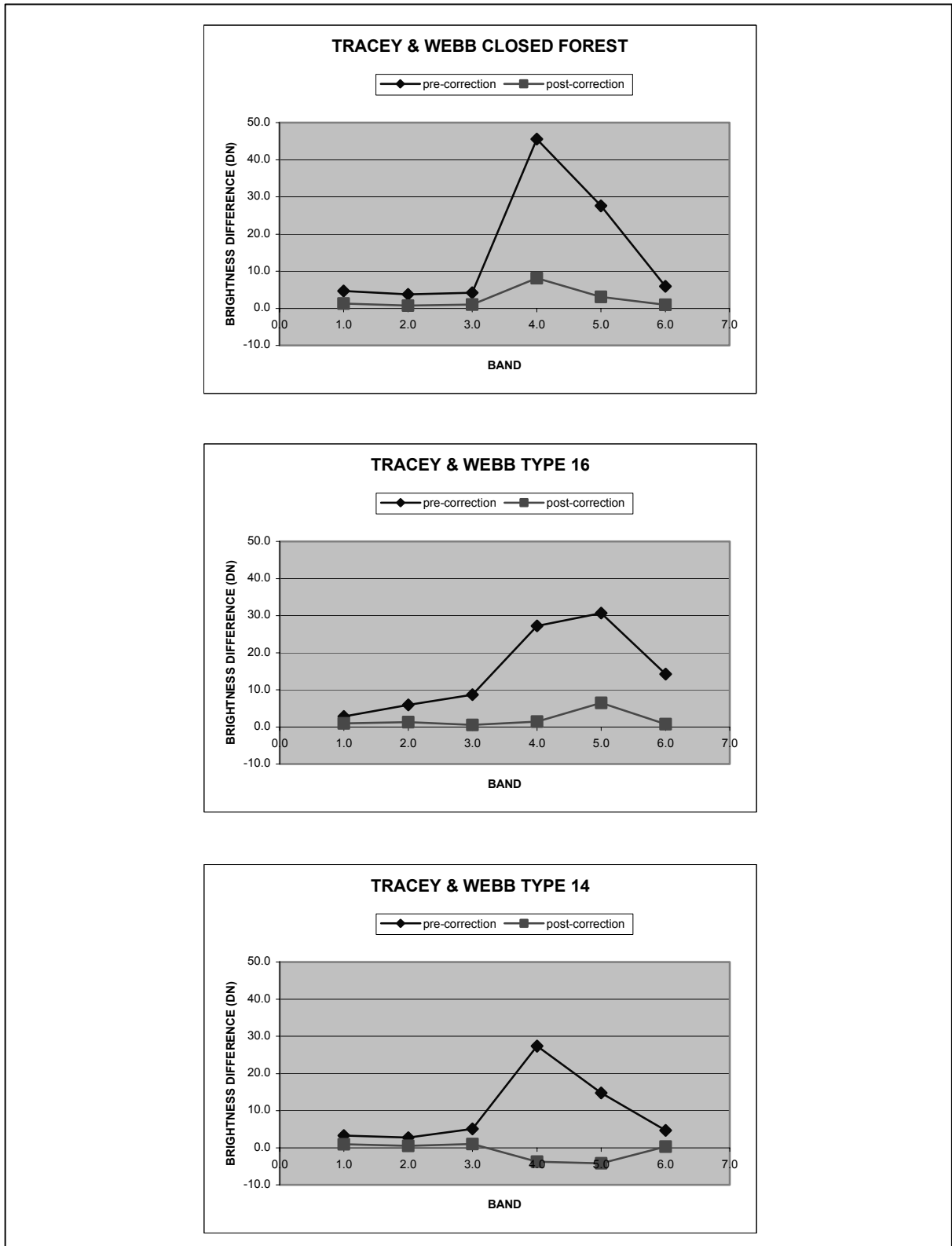


Figure 16: Radiometric accuracy for each band for scene 9673, era 1999, expressed as the average brightness difference between spectral signatures of Areas of Interest (AOIs) from both shaded and sunlit areas prior to and post topographic normalisation, for representative Tracey and Webb vegetation communities as determined from Stanton and Stanton (2005).

4.4. RELATIVE RADIOMETRIC CORRECTION

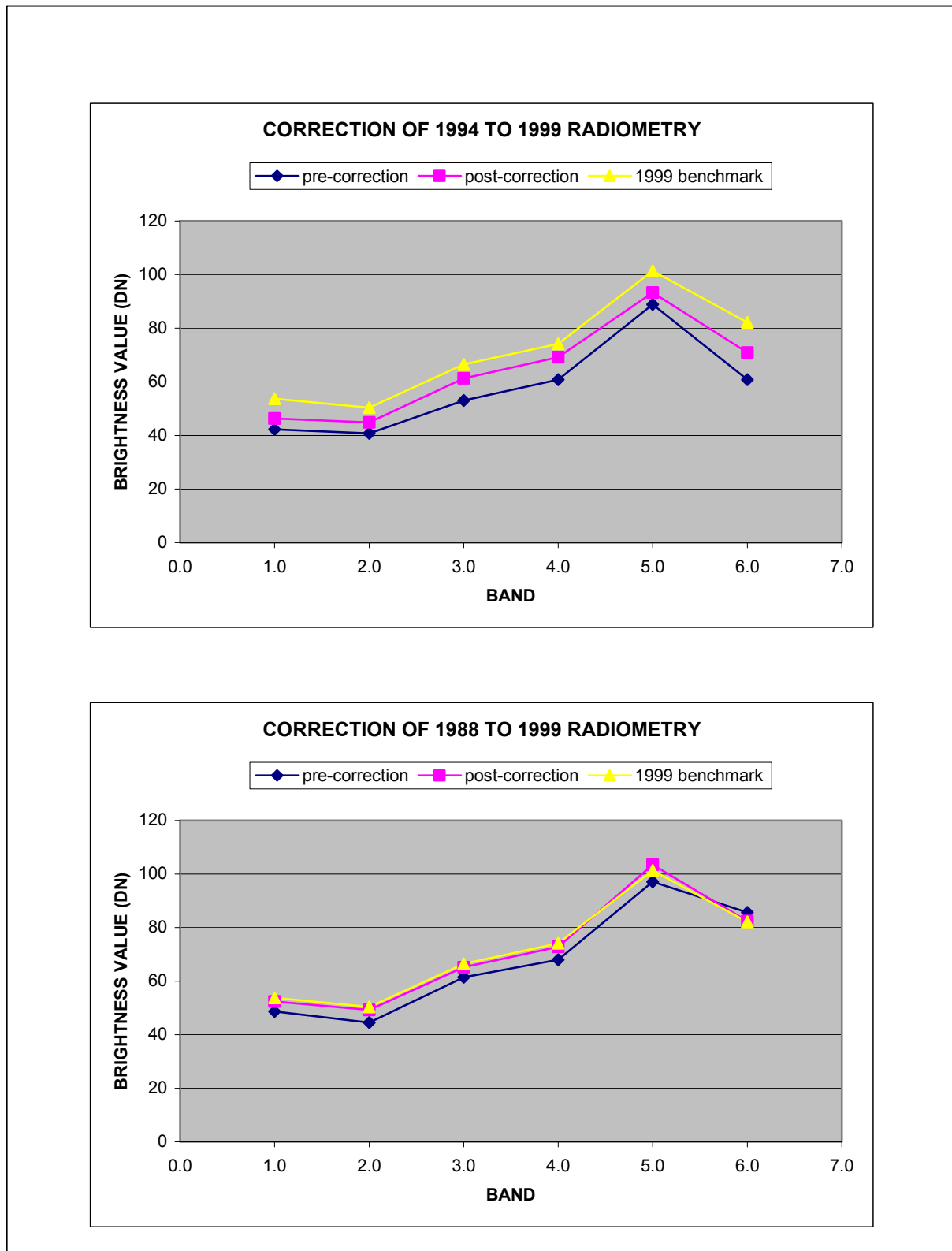


Figure 17: Relative radiometric accuracy for each band for each mosaic, expressed as the average brightness of spectral signatures of Pseudo-Invariant Features (PIFs) spread across the 1988 and 1994 image mosaics, prior to and post radiometric correction to the 1999 image mosaic standard.